

10498

NACA TN 4159

0067033



TECH LIBRARY KAFB, NM

# NATIONAL ADVISORY COMMITTEE FOR AERONAUTICS

TECHNICAL NOTE 4159

EXPERIMENTAL INVESTIGATION OF TURBOJET-ENGINE MULTIPLE-  
LOOP CONTROLS FOR NONAFTERBURNING AND AFTERBURNING  
MODES OF ENGINE OPERATION

By Donald B. Kirsch, Leon M. Wenzel, and Clint E. Hart

Lewis Flight Propulsion Laboratory  
Cleveland, Ohio



Washington  
January 1958

AFMDC  
TECHNICAL LIBRARY  
AFL 2311



## NATIONAL ADVISORY COMMITTEE FOR AERONAUTICS

## TECHNICAL NOTE 4159

EXPERIMENTAL INVESTIGATION OF TURBOJET-ENGINE MULTIPLE-LOOP CONTROLS  
FOR NONAFTERBURNING AND AFTERBURNING MODES OF ENGINE OPERATION

By Donald B. Kirsch, Leon M. Wenzel, and Clint E. Hart

## SUMMARY

An experimental investigation of turbojet-engine performance with several configurations of interacting multiple-loop controls was conducted to determine the mode of control required for obtaining optimum rotor speed and turbine-discharge temperature transient response characteristics during (1) thrust increase and (2) afterburner ignition by manipulation of engine fuel flow and exhaust-nozzle area. The engine operating point chosen for examining the control systems was near the rated-thrust level.

Effective increases in engine thrust were obtained by rapidly opening the nozzle area while simultaneously increasing engine fuel flow. Following the afterburner ignition, opening the nozzle area rapidly while holding an essentially constant engine fuel flow practically eliminated compressor surge tendencies. Good engine transient performance characteristics were obtained with a control system in which engine speed was controlled by manipulation of exhaust-nozzle area and turbine-discharge temperature was controlled by manipulation of engine fuel flow.

An alternate control system, which gives acceptable although more oscillatory transient responses, was the double-loop configuration in which speed was controlled by manipulation of engine fuel flow, turbine-discharge temperature was controlled by manipulation of exhaust-nozzle area, and a noninteraction gain term was incorporated from the speed to the temperature control loops.

## INTRODUCTION

The demand for more exacting engine transient performance characteristics has emphasized the importance of a fast-acting variable-area exhaust nozzle and its function as a primary controlling parameter. During normal engine operation a modulating exhaust nozzle may be used to advantage by allowing a rapid thrust increase, maximum thrust at

various engine operating conditions, or the best specific fuel consumption at different power levels. Further, the application of afterburning to the turbojet engine implicitly requires the use and control of a variable-area exhaust nozzle. This report investigates some of the modes of closed-loop controls that are possible by manipulation of the two independent engine variables, engine fuel flow and exhaust-nozzle area.

Two of the turbojet-engine output variables, rotor speed and turbine-discharge temperature, must be limited or controlled to prevent engine surge, failure, or damage; overspeed or overtemperature conditions may result when operating the engine near the rated-thrust level. Consequently, various multiple-loop linear control systems were examined for optimizing the speed and temperature transient responses during (1) the transition from a lower to a higher thrust level by simultaneously calling for step increases in set rotor speed and set turbine-discharge temperature and (2) a simulated afterburner ignition. The control problems encountered during starting and acceleration from idle and cruise conditions were not considered.

In preparation for the multiple-loop-control studies contained herein, comprehensive experimental investigations were made to define the specific nature of single-loop controls on a turbojet engine. In particular, the speed-area, speed - fuel-flow, temperature-area, and temperature - fuel-flow control loops were examined individually, and the results are presented in references 1 and 2. The engine apparatus, instrumentation methods, and control techniques developed during these investigations are utilized in the present experimental study.

## APPARATUS

### Engine

The control tests were conducted on a turbojet engine that incorporated a 13-stage axial-flow compressor, vaporizing-type fuel injectors, an annular-shaped combustor, a two-stage turbine, and a variable-area exhaust nozzle. The engine was installed in a sea-level static test cell.

### Fuel System

The original fuel system of the engine, with the exception of the manifold and flow dividers, was replaced with a research facility fuel control described in reference 3. The fuel control consisted of a reducing-type differential pressure regulator that maintained a constant pressure drop across the throttle valve and an electrohydraulic servo

system to vary the throttle-valve position. The resulting fuel flow was proportional to the throttle-valve position.

Frequency response data show that the throttle-valve position in relation to the input signal had an amplitude response essentially flat to beyond 10 cycles per second and a dead time of approximately 0.005 second.

#### Exhaust Nozzle

The variable exhaust nozzle, described fully in references 1 and 2, was designed to give good frequency response characteristics; the thrust coefficient with this nozzle, however, was low.

The nozzle-area variation obtained was 73 to 113 percent of rated area. Steady-state area variation was nearly linear with input signal to the electrohydraulic power system; frequency response characteristics of the nozzle-area mechanism from reference 1 are shown in figure 1.

### INSTRUMENTATION

#### Engine Speed

A measure of instantaneous engine speed was obtained with a magnetic pickup and an electronic circuit that converted the frequency signal to a direct-current signal proportional to the number of voltage pulses per unit time. The magnetic pickup was mounted in the compressor housing opposite steel rotor blades. The electronic circuit had no measurable dynamics in the frequency range of interest.

For steady-state speed measurement, a digital counter displayed actual engine speed.

#### Tailpipe Temperature

Four rakes, each consisting of four Chromel-Alumel thermocouples, were used for measuring transient tailpipe gas temperature. The rakes were located around the periphery of the tailpipe in order to obtain a representative cross-sectional temperature.

As a compromise between fast response and durability, 22-gage wire was used for these thermocouples which gave a thermocouple time constant of approximately 0.30 second in the region of engine operation selected for the control study.

Thermocouples on two additional rakes, similar to the ones used for transient measurement, were connected to a self-balancing potentiometer for steady-state temperature measurements.

#### Fuel Flow

A linear differential transformer connected to the throttle valve gave a signal indicative of fuel flow during transients.

Steady-state fuel-flow measurements were obtained with a rotameter.

#### Exhaust Nozzle

A rotary differential transformer connected to the area mechanism gave a signal indicative of the effective area during transients.

Steady-state area measurements were indicated on a precision meter that measured the voltage on the arm of a linear wire-wound potentiometer connected to the mechanism.

#### Recording Equipment

Transient data were recorded on a direct-writing six-channel oscillographic recorder. The recorder pens, when used with equalizing amplifiers, had a frequency response essentially flat to 100 cycles per second. A recorder chart speed of 25 millimeters per second was used (0.2 sec per division).

#### Analog Computing Equipment

Circuits for calculating time integrals of the square of the speed errors and temperature errors were set up by using linear and nonlinear elements of an electronic analog computer. The proportional-plus-integral controller elements of the closed-loop configurations were also obtained with the computer.

### CONTROL SYSTEMS

When rotor speed and turbine-discharge temperature are the controlled parameters, two basic double-loop control systems can be utilized on a turbojet engine since both parameters are functions of engine fuel flow and exhaust-nozzle area. Each of the basic control systems (1) speed-

area, temperature - fuel-flow and (2) speed - fuel-flow, temperature-area with certain modifications is studied in this report in order to determine the engine stability and transient response characteristics.

The process of control may be visualized as computing the rotor speed and turbine-discharge temperature error signals and correcting with proportional-plus-integral controller action  $K\left(1 + \frac{1}{\tau s}\right)$ . (All symbols are defined in appendix A.) The resulting signals were then applied to the control servos to vary nozzle area and engine fuel flow simultaneously until the speed and temperature errors became zero.

In the two basic turbojet-engine control systems, engine interaction exists between the controlled variables and may be favorable or unfavorable to the over-all system transient characteristics. In order to partially compensate for the engine interaction effects with the intent of improving system performance, gain term elements were added between the forward paths of the control loops and were adjusted until the engine interaction was minimized. Further discussion of noninteraction control theory is presented in references 4 and 5.

#### Speed-Area and Temperature - Fuel-Flow Control Systems

A diagram of the speed-area, temperature - fuel-flow control system with noninteraction gain terms is shown in figure 2(a). The action of the basic configuration was examined with (1) no compensation, (2) speed - fuel-flow compensation through the  $K_{n/t}$  gain term, and (3) temperature-area compensation through the  $K_{t/n}$  gain term.

#### Speed - Fuel-Flow, Temperature-Area Control Systems

Similarly, a diagram of the speed - fuel-flow, temperature-area control systems with noninteraction gain terms is shown in figure 2(b). The action of the basic configuration was examined with (1) no compensation, (2) speed-area compensation through the  $K_{n/t}$  gain term, and (3) temperature - fuel-flow compensation through the  $K_{t/n}$  gain term.

The block diagram and response equations for these double-loop control configurations are discussed in appendix B. The dynamic characteristics of all the system components in the block diagram were obtained from sinusoidal frequency response data presented in references 1 and 2 and, for convenience, are tabulated in table I.

## PROCEDURE

## Thrust Increase Study

The testing procedure consisted of applying simultaneous step inputs in set speed and temperature to the control systems shown in figure 2 and recording the responses of engine variables as a function of controller gains, controller time constants, and noninteraction gain. Time integrals of the square of speed and temperature errors were also taken to gage the transient performance of the system.

The initial and final engine steady-state operating levels are indicated by points A and B, respectively, on the engine operating map in figure 3. The steps taken were +3.0 percent of rated speed and +6.2 percent of rated temperature from the initial operating levels of 94-percent rated speed (rpm) and 85.4-percent rated temperature ( $^{\circ}\text{R}$ ). These steps resulted in steady-state changes of +13.0 percent of rated fuel flow (lb/hr) and -1.33 percent of rated exhaust-nozzle area (sq in.) for engine operation at the new thrust level.

Stability studies were made on two control systems by determining the controller settings required to cause system instability and verifying these settings with sinusoidal frequency response data given in references 1 and 2. The results of the stability studies are presented in appendix B.

## Afterburner Ignition Study

A procedure for simulating the pressure buildup accompanying an afterburner ignition was used to obtain speed, temperature, and compressor-discharge pressure transients that would result from an instantaneous afterburner ignition. This procedure consisted of introducing a step signal directly to the area servo, which caused an immediate partial closing of the exhaust-nozzle area. The control system then brought the speed and temperature variables back to their original values by manipulation of the engine fuel flow and exhaust nozzle.

The disturbance normally encountered during an actual afterburner ignition is equivalent to a decrease in the nozzle area of approximately 40 percent of rated at static sea-level conditions. Since this is a severe disturbance, a decrease in the exhaust-nozzle area of only 10 percent of rated was chosen to facilitate the study of the engine transient performance with a large number of controller settings in the various control configurations.

The testing procedure for examining control action in response to a simulated afterburner ignition consisted of adjusting the controller

gain settings to obtain the best transient characteristics; the controller integrator settings and the noninteraction gain values chosen for the thrust increase study were held constant for this part of the investigation.

## RESULTS AND DISCUSSION

### Increasing Engine Thrust by Simultaneously Increasing Operating

#### Levels of Rotor Speed and Turbine-Discharge Temperature

Transient performance criterion. - Adjustment of the system controller settings suggests the use of an integral performance criterion to minimize the areas under the system response curves and to aid in comparing the behavior of the various control configurations. Of the minimizing integral criteria available for evaluating transient responses, the integral of the error squared was selected for this study.

In order to optimize the system transients, the closed-loop step response data were analyzed to define the actual performance of the system in terms of transient overshoots and solution times. The controlled system for which the overshoots and solution times were jointly minimized is herein defined as optimum.

Speed-area, temperature - fuel-flow control system with no compensation. - In reference again to the block diagram in figure 2(a), simultaneous step increases in set speed and temperature,  $+\Delta N_s$  and  $+\Delta T_s$ , were applied to the control loops. With the noninteraction gains  $K_{n/t}$  and  $K_{t/n}$  reduced to zero, the proportional and integrator settings in both controllers were adjusted to achieve the best speed and temperature transient responses.

In order to determine the optimum combination of integrator settings in the proportional-plus-integral controllers  $K\left(1 + \frac{1}{\tau_s}\right)$ , the envelopes of a series of plots similar to the one shown in figure 4(a) are summarized in figure 4(d). In the summary plot the minimum temperature performance integral  $\int T_e^2$  is plotted against the speed performance integral  $\int N_e^2$  for several combinations of controller integrator settings. Before deciding upon the optimum controller integrator settings, it is desirable to examine one of the performance integral plots in detail.

In figure 4(a), curves of temperature performance integrals  $\int T_e^2$  plotted against the speed performance integrals  $\int N_e^2$  are shown as lines

of constant speed controller gain  $K_n$  and lines of constant temperature controller gain  $K_t$  for integrator settings of  $\tau_n = \tau_t = 0.50$  second. The significance of the integral performance plots becomes apparent by examining the slopes and minimizing tendencies of the curves. With low speed and temperature controller gain settings,  $K_n = 1.0$  and  $K_t = 0.0625$ , poor responses are realized in both output parameters as indicated by the large  $\int T_e^2$  and  $\int N_e^2$  values. Proceeding along the constant  $K_n = 1.0$  line by progressively increasing the  $K_t$  value, both performance integrals decrease until the temperature response optimizes at a  $K_t$  value of 0.100. The diagonal slopes of the constant  $K_n$  lines are due to interaction within the engine between the temperature and speed loops. Increasing the temperature-loop gain increases the engine fuel flow during the transient which permits a faster engine acceleration and a corresponding decrease in  $\int N_e^2$ . In an attempt to decrease the  $\int N_e^2$  still further, the speed-area controller gain  $K_n$  was continually increased until the entire performance grid was obtained. While increasing  $K_n$  to lower the speed performance integral, a slight sacrifice is made in temperature performance as indicated by the negative slopes of the constant  $K_t$  lines. It follows that the interaction effects of nozzle-area movement are unfavorable to temperature response. In order to establish the lowest performance integral values for a given combination of controller integrator settings, a curve may be drawn connecting the minimum temperature integrals for each value of speed controller gain setting. For these curves of  $\tau_n = \tau_t = 0.50$  second, the envelope of the plot is nearly the constant  $K_t$  line of 0.100.

A series of similar envelope curves are shown in figure 4(d) for various integrator settings. From this summary plot, the following boundary conditions can be shown to exist for optimum speed response:

$$0.50 < \tau_n < 1.0$$

and

$$0.50 < \tau_t < 1.0$$

Also, for optimum temperature responses:

$$0.25 < \tau_n < 0.50$$

and

$$0.50 < \tau_t < 1.0$$

It may be concluded from these results that in addition to proportional gain some integral action is also required in the controller for obtaining optimum output responses. At the engine thrust level chosen for this investigation, the engine time constant was linearized at 0.83 second. The minimum controller integrator settings required for these operating conditions were 0.25 second in the speed-area loop and 0.50 second in the temperature - fuel-flow loop.

In order to verify the use of the error squared integral minimum as a satisfactory method for determining the optimum integrator settings, the engine transient response traces were analyzed for percent overshoot and 10-percent settle-out times. The optimum integrator settings determined with the transient data were in good agreement with those determined from the integral criterion.

A region of satisfactory transient responses may be established by minimizing both the speed and temperature performance integrals. Speed and temperature transient analysis data are plotted for such a case in figures 4(b) and (c). The portion of the performance integral grid examined in these figures is bounded by a speed controller gain of greater than 2.0 and a temperature controller gain of approximately 0.075 to 0.100. Controller gain in the speed-area loop was not increased beyond 8.0 to prevent erratic area movements caused by the noise content of the speed signal. Considerable information can be obtained from these plots and also from oscillographic recordings representative of actual engine performance (figs. 4(e) and (h)). These transient recordings are located on the transient data plots (figs. 4(b) and (c)) by solid symbols.

The transient recordings show rotor speed error and indicated turbine-discharge temperature-error responses together with fuel-flow and exhaust-nozzle-area changes. The increasing and opening directions are indicated by arrows and plus signs. Sensitivities are noted in percent of rated engine values per millimeter. Transient overshoot and 10-percent settle-out time are defined on the speed-error trace in figure 4(e).

Figure 4(e) shows the system performance with low controller gains in both the speed-area and temperature - fuel-flow loops. The step disturbances in set speed and temperature appear in the error traces as immediate positive error signals. Fuel flow increases according to the proportional-plus-integral controller action while the exhaust-nozzle area momentarily limits at the maximum preset value. These conditions are ideal for fast rotor acceleration which takes place after the relatively short speed-area dead time (0.021 sec). A considerable time delay, however, is observed before the indicated temperature begins to increase. This delay is due to an opening of the nozzle area, tending to lower temperature, the dead times associated with fuel-flow transport and combustion (0.083 sec), and the thermocouple time constant (0.30 sec). Because of the delayed temperature response there is an excess quantity of engine

fuel flow, which makes the adjustment of the temperature - fuel-flow controller settings critical for obtaining optimum system performance.

Figure 4(f) shows the engine performance obtained with a high speed-area loop gain and a low gain setting in the temperature - fuel-flow controller. Increasing the speed-area gain improved speed performance by decreasing overshoot and solution time; temperature response remained essentially the same. It should be noted that with a limited nozzle-area excursion, the speed response was improved substantially by tightening the control in the speed-area loop. To increase the rate of rotor acceleration further, additional energy must be supplied to the system by increasing the temperature controller gain, which causes greater fuel-flow changes as shown in figures 4(g) and (h). Both loops are operated with a high controller gain in figure 4(g) and show the temperature response to be oscillatory. This trace shows the ability of a fast-acting nozzle-area mechanism to control speed in the presence of a fluctuating engine fuel flow.

Figures 4(b) and (c) show the speed and temperature performance characteristics for various values of controller gain settings. Plots of this type are useful in optimizing the transient behavior of the controlled parameters and in predicting the range over which the controller gains may be varied without sacrificing system performance. The curves appear as constant  $K_n$  and  $K_t$  lines similar to those in the performance integral plots.

Figure 4(b) shows that, for a constant  $K_t$  value, increasing the speed controller gain  $K_n$  improves the speed performance by lowering overshoot and reducing solution time. The presence of control-loop interaction is evidenced by the spacing between the lines of constant temperature controller gains  $K_t$ . The major interaction effect of increasing  $K_t$  is to increase speed overshoot which is in part due to a larger initial engine fuel-flow burst. A nonlinear effect is introduced into the control configuration during the early part of the transient because of the limiting nozzle area. The interaction between fuel flow and engine speed would be decidedly less than that observed if the area were fully modulating following the disturbance.

The temperature performance plot (fig. 4(c)) shows that, with a low temperature controller gain setting, the lines of constant  $K_n$  converge and nozzle-area interaction is reduced to a minimum. Adjustment of  $K_t$ , however, is critical because temperature overshoot and settle-out time increase with temperature-loop gain.

The single-loop engine control studies point out that the speed-area control loop is inherently stable over a large range of loop gains. This

fact becomes a practical design feature when considering multiple-loop control configurations and the permissible latitude of controller adjustment. Since indicated turbine-discharge temperature is relatively insensitive to nozzle-area changes, coupled with the fact that rotor speed performance continues to improve with an increasing speed-area loop gain, the use of a fast-acting nozzle area controlled with a speed-error signal is recommended.

Using the transient analysis data plots and comparing the system performance characteristics shown in oscillographic traces permit a choice of controller gain settings to be made for optimum speed and temperature responses. Such a choice is shown in figure 4(h) in which a high speed-area controller gain is employed with an intermediate value of temperature - fuel-flow controller gain.

A study of the stability characteristics for this control system is presented in appendix B. The results show that the components in the temperature - fuel-flow control path are critical for determining system stability.

Speed-area, temperature - fuel-flow control system with speed - fuel-flow compensation. - In the integral performance plot for the basic double-loop system (fig. 4(a)), engine interaction was shown to be slightly unfavorable to temperature performance. In order to minimize the effects of this interaction, a gain term was connected between the forward paths of the two loops (gain  $K_n/t$  in fig. 2(a)) and was adjusted to give the least temperature deviation for a change in set speed. The control modification caused an additional increase in engine fuel flow to cancel the effects of an opening exhaust-nozzle area on turbine-discharge temperature.

The integral performance and transient analysis data curves for this control configuration are presented in figures 5(a) to (c). The slopes of the constant  $K_t$  lines in the integral plot indicate that by adding the speed - fuel-flow compensation term to the basic system the temperature and speed performance integrals are both improved by increasing the speed-area loop gain. Similarly, the performance integrals are improved by increasing the temperature - fuel-flow loop gain.

The transient performance curves in figures 5(b) and (c) show the region on the integral plot bounded by a  $K_n$  greater than 2.0 and a  $K_t$  of approximately 0.050 to 0.070. In choosing the optimum controller gain settings from these plots, it is necessary to compromise the speed and temperature settle-out times which appear to be mainly a function of  $K_n$ . The  $K_t$  setting has relatively less effect on speed response and may be adjusted to minimize the temperature overshoot.

4476

CP-2 back

In order to compare the results of using a high or low value of speed-area loop gain, two oscillographic traces are presented in figures 5(d) and (e). The temperature - fuel-flow controller gain setting was nearly an optimum value for both of these response traces. In figure 5(d) excellent speed response characteristics are realized with a high  $K_n$  value; the temperature response, however, is shown to be oscillatory. Decreasing the speed-area loop gain to a lower value imposes a slight sacrifice on the speed solution time, but, as shown in figure 5(e), the temperature transient response is considerably improved.

Speed-area, temperature - fuel-flow control system with temperature-area compensation. - With this control system an attempt was made to partially compensate for the effects of an engine fuel-flow change on speed response by simultaneously manipulating the nozzle area. The compensation afforded by the gain term was not completely satisfactory because of the differences in the speed-to-area and speed-to-fuel-flow dead times.

The integral performance criteria and transient analysis data curves for this system are presented in figures 6(a) to (c). Examination of the integral curves for the two disturbances indicate that the temperature-area gain term was most effective for a  $K_n$  value of approximately 2.0. Increasing or decreasing the speed-area loop gain about this value resulted in a fuel-flow - speed interaction as shown by the sloping of the lines of constant-speed controller gains.

The transient performance curves in figure 6(b) and (c) show the speed response characteristics to be essentially the same as those obtained with the basic double-loop configuration. Temperature performance is excellent when the system is operated at a low  $K_n$ , but speed response is poor. As  $K_n$  is increased, temperature solution time and overshoot increase (fig. 6(c)).

The opposing nature of the two signals controlling the movement of the exhaust-nozzle area explains the abrupt change in the lines of constant  $K_t$  shown in figure 6(c). With  $K_n < 2.0$ , the temperature-area signal causes an initial closing of the nozzle area which favors the temperature response at the expense of speed solution time and overshoot. With  $K_n > 2.0$ , the speed error becomes the predominating signal and causes an initial opening of the area following the input disturbances.

An oscillographic trace representative of engine performance is presented in figure 6(d). Introducing the simultaneous step input commands causes fuel flow to increase and nozzle area to open. Close examination of the traces reveals that the magnitude of the speed-area signal completely obscures the temperature-area signal in manipulating the nozzle area.

Speed - fuel-flow, temperature-area control system with no compensation. - In the present section of the report transient performance with the second type of double-loop control is examined. The control-system block diagram is shown in figure 2(b) in which speed is controlled by manipulation of fuel flow and temperature is controlled by manipulation of exhaust-nozzle area. The noninteraction gain terms  $K_n/t$  and  $K_t/n$  were set to zero.

The integral performance criteria and transient analysis data are plotted in figures 7(a) to (c). Comparing figure 7(a) with figures 4(a), 5(a), and 6(a) indicates unsatisfactory speed and temperature transient characteristics. The factors contributing to the large performance integral values are long speed solution times and extreme temperature overshoots which are shown by the curves in figures 7(b) and (c).

An oscillographic recording of engine performance with this control system is presented in figure 7(d). An appreciable delay in rotor acceleration occurs which permits an excess amount of engine fuel flow and results in extreme overtemperature conditions.

Comparing the data for the two basic control systems leads to the conclusion that nozzle-area movement has a greater effect in controlling speed than in regulating temperature during the transients. This fact suggests that a speed-area compensation should be included in the speed - fuel-flow, temperature-area control configuration to improve the speed performance and, indirectly, to improve temperature transient characteristics. The compensation would cause an initial opening of the nozzle area and permit the rotor to accelerate faster which would reduce the net quantity of engine fuel flow. The results of this modification to the basic double-loop configuration are presented in the following section.

Speed - fuel-flow, temperature-area control system with speed-area compensation. - With the speed-area noninteraction gain term adjusted to give the least temperature deviation for a small step change in set speed,  $+\Delta N_s$  and  $+\Delta T_s$  input disturbances were applied to the control loops to obtain the minimum integral curves presented in figure 8(a). From the curves it may be concluded that controller integrator action of  $\tau_n = 0.50$  second or greater and  $\tau_t = 0.25$  second or greater is required for minimizing the speed and temperature performance integrals. Of special interest are the minimum criteria values which imply that the transient characteristics for this control are directly comparable with those obtained with the speed-area, temperature - fuel-flow controls.

The integral performance criteria and transient analysis data are plotted for controller time constants of  $\tau_n = 0.50$  second and  $\tau_t = 0.25$  second in figures 8(b) and (c). The slopes of the constant  $K_t$  and  $K_n$

lines in the integral plot indicate the presence of engine interaction between the control loops. The physical nature of the interaction effects is best illustrated in the transient data plots which show speed overshoot and solution time to increase with an increasing  $K_t$  and temperature solution time to decrease with an increasing  $K_n$ . Speed and temperature overshoot and solution time increase rapidly with  $K_t > 0.30$ . Increasing  $K_n$  beyond 2.0 resulted in an oscillatory engine fuel flow and underdamped transient responses. The stability characteristics for this control system are examined in appendix B.

Oscillographic recordings representative of engine performance are presented in figures 8(e) to (g). The traces show the effect of progressively increasing the temperature-area controller gain setting on the time histories of the various engine parameters. With a low  $K_t$  value (fig. 8(e)) the area and fuel-valve servos move in a manner to favor the speed response; temperature, however, is slow to reach steady-state solution time. Increasing the  $K_t$  gain setting (fig. 8(f)) tightens the temperature-area control and improves the temperature response. Increasing the  $K_t$  gain setting still further (fig. 8(g)) shows the effect of the two opposing error signals in controlling the area movement. Both speed and temperature overshoots are higher, and the system shows an increased tendency to oscillate. The operating conditions for the performance characteristics shown in figure 8(f) were chosen as optimum.

Speed - fuel-flow, temperature-area control system with temperature - fuel-flow compensation. - The speed and temperature integral performance criteria and transient analysis data are plotted in figures 9(a) and (b). The grid network location on the integral performance plot implies that adding the temperature - fuel-flow noninteraction gain term to the basic control (fig. 7(a)) improves temperature performance but causes a sacrifice in speed response. The overshoot and 10-percent solution time curves show that temperature overshoot was substantially lowered, while speed solution time was slightly increased.

An oscillographic recording of engine performance with this control is presented in figure 9(c). Following the initial  $+\Delta N_g$  and  $+\Delta T_g$  input commands, control action causes a closing of the nozzle area and a large engine fuel-flow burst. The combination of these two actions produces a high temperature overshoot and an appreciable delay before the engine begins to accelerate. The performance characteristics with this control are very similar to the basic system with the exception that speed is slow in reaching the final steady-state value and that there is virtually no speed overshoot.

4476

Comparison of control systems investigated. - A series of oscillographic recordings were compiled in figure 10 to compare the optimum performance characteristics for each of the control configurations investigated. The traces in the recordings were normalized and overlaid on rectilinear coordinates to facilitate evaluating the transients and servo movements.

For the specific control requirement of simultaneously increasing the engine speed and temperature operating levels in the best manner, two control configurations may be eliminated immediately on the basis of the transients shown in figure 10(b). Overtemperature and overspeed conditions are evidenced by the transients for the speed - fuel-flow, temperature-area control systems with no compensation and with temperature - fuel-flow compensation. Comparing the transients for the remaining four systems shows that all the responses are very similar in nature, except for discrete variations in overshoot or solution time. The similarities are due in part to the initial movements of the engine fuel-valve and exhaust-nozzle-area servos as shown in the same figures.

Very little difference exists among the servo movements for the speed-area, temperature - fuel-flow controls in figure 10(a). Comparing the curve in figure 10(b) for the speed - fuel-flow, temperature-area control system with speed-area compensation to the traces in figure 10(a) shows a reduction in the maximum engine fuel flow and a lesser nozzle-area movement. The area is required to open rapidly, but the closing action may be rate-limited. Transientwise, the net effect of these reduced servo motions is a longer speed solution time.

#### Simulated Afterburner Ignition

Analysis of afterburner ignition data. - The control action of the multiple-loop configurations was investigated by observing rotor speed, turbine-discharge temperature, and compressor-discharge pressure variations following the simulated afterburner ignition. The engine control objectives were to reduce compressor surge tendencies and eliminate possible turbine blade damage by effectively manipulating engine fuel flow and exhaust-nozzle area.

Two types of plots were used to evaluate and compare the speed and temperature transients. In the first type, speed undershoot and temperature overshoot were plotted for various values of controller gain settings. The performance criterion for these curves was to minimize the variation of both output parameters.

The second approach used to evaluate the control systems was to predict compressor surge tendencies from curves of maximum compressor-discharge pressure deviation plotted against rotor speed undershoot for

various values of controller gain settings. These plots gave a qualitative measure of compressor operation during the transient as determined by engine steady-state data. Engine steady-state performance maps show compressor-discharge pressure to decrease with rotor speed to maintain a certain compressor surge margin. This fact, when applied to the afterburner transient data, served as a general performance criterion for the control systems.

Speed-area, temperature - fuel-flow control systems. - The afterburner transient data for the speed-area, temperature - fuel-flow basic control configuration are presented in figures 11(a) and (b). Curves of rotor speed undershoot are plotted against speed controller gain settings in figure 11(a) for a high and a low value of temperature controller gain. The amount of speed undershoot is reduced by increasing the speed controller gain setting and lowering the gain in the temperature - fuel-flow loop. The presence of engine interaction causes a slight separation in the lines of constant temperature controller gain that is due to a temperature increase following the disturbance.

The relatively passive effect of the temperature - fuel-flow control loop on speed response may be explained by examining the indicated temperature and fuel-valve oscillographic traces in figure 11(c). These traces illustrate optimum system performance with controller gain settings of  $K_n = 4.0$  and  $K_t = 0.075$ . At the initial command the nozzle area is instantaneously decreased to introduce the load disturbance. The nozzle area is moved back to the initial steady-state position by the speed-area control action. The magnitude of the temperature deviation following the load disturbance is barely separable from the signal noise level. Consequently, engine fuel flow remains essentially constant.

At this point, it is of interest to examine an oscillographic trace illustrating unsatisfactory engine performance with this control system. Figure 11(d) shows adverse operating conditions resulting from a low  $K_n$ , which causes the area to open slowly, and a high  $K_t$ , which prompts a discernible decrease in engine fuel flow. A decreasing rotor speed and a slowly opening area lead to increasing temperature conditions as indicated by the traces. A possible disadvantage with this control configuration if a rate-limited variable nozzle area mechanism were used is that overtemperature conditions may cause engine fuel flow to decrease to such a level that speed performance would be seriously affected.

A closer examination of the responses in the two figures reveals that nearly the entire control recovery action is due to the nozzle-area movement since engine fuel flow remains practically constant. These data suggest a simplified version of this control system for afterburner ignition that would consist of a single-loop speed-area control.

In order to examine the speed - compressor-discharge pressure relation following the afterburner ignition, rotor speed undershoot was plotted against maximum compressor-discharge pressure deviation in figure 11(b) for various values of controller gains. The constant  $K_n$  and  $K_t$  grid network is located in a region on the figure in which compressor-discharge pressure decreases with rotor speed. These curves indicate that, although the possibility of compressor surge may not be entirely eliminated, the engine operating conditions that favor compressor surge are reduced to a minimum.

The effects of adding the speed - fuel-flow noninteraction gain term to the basic control configuration were partially investigated. The results showed that the noninteraction gain value used for the study was not large enough to cause a substantial change in the performance of the basic system. Increasing the speed - fuel-flow noninteraction gain, however, could serve as one method of canceling the temperature - fuel-flow effect if the engine were equipped with a rate-limited variable nozzle area.

The effects of adding the temperature-area noninteraction gain term were also investigated. The results showed that with this engine unit the compensation signal did not cause any marked difference in the performance of the basic control system. With an engine equipped with a slower nozzle area, a greater temperature deviation would be experienced. In this case, a temperature compensation signal would be influential in controlling the area and, most likely, improving system performance.

Speed - fuel-flow, temperature-area control systems. - The transient performance criteria are plotted as a function of controller gain settings in figures 12(a) and (b) for the three control configurations investigated with the speed - fuel-flow, temperature-area double-loop control system.

The temperature overshoot and speed undershoot curves (fig. 12(a)) show that overtemperature conditions present a major control problem. A representative oscillographic trace of engine performance with the basic control configuration is presented in figure 12(c). This trace illustrates the ineffectiveness of the basic control in recovering the engine from the disturbance as evidenced by the large speed and temperature fluctuations. The control process may be visualized as the speed-error signal causing an increase in engine fuel flow while the temperature error is tending to open the nozzle area. An appreciable time delay, which is observed before the indicated temperature begins to increase, permits the area to remain, in effect, uncontrolled for approximately 0.20 second. During this time, rotor speed continues to drop, and engine fuel flow is increased accordingly. Engine interaction between the control loops produces transient responses that are highly oscillatory.

An improvement in the temperature transient performance may be realized by incorporating a temperature - fuel-flow noninteraction gain term in the basic control configuration. The action of the compensation is to oppose the speed - fuel-flow signal and thereby reduce the initial engine fuel-flow burst following the disturbance. The curves in figure 12(a) show that the temperature - fuel-flow modification reduces temperature overshoot, but with a sacrifice in speed performance. An oscillographic trace for this system is presented in figure 12(d). Comparing these traces with those in figure 12(c) shows that adding the compensation eliminates the oscillatory characteristics of the system and reduces the variation in compressor-discharge pressure. Here it should be noted that the outstanding differences among the performances of these systems and those examined in the previous section lie, in particular, with the slowly opening area and the dependence upon fuel flow for the engine recovery.

The results of adding a speed-area noninteraction gain term to the basic system are shown in figure 12(a). This modification, in addition to reducing the speed undershoot to a value that was comparable to that in the speed-area, temperature - fuel-flow control systems, minimized the overtemperature conditions as well. The working action of the compensation term may be observed by studying the oscillographic traces in figure 12(e). The speed-error signal causes an engine fuel-flow burst and a rapidly opening nozzle area. Performance-wise, the temperature overshoot obtained herein is not objectionable, but speed response is oscillatory and, consequently, undesirable. Comparing the curves in this figure with those in figure 11(c) for the speed-area, temperature - fuel-flow control system shows that the engine can be adequately recovered from the disturbance without the aid of an increasing engine fuel flow.

The plots of compressor-discharge pressure variation and speed undershoot in figure 12(b) indicate the compressor surge characteristics for these control systems. The curves indicate that the temperature - fuel-flow compensation control system gives the greatest margin from the compressor surge region, but at the expense of considerable speed undershoot. The compressor surge tendencies with the speed-area compensation are still present although considerably reduced from those of the basic system.

#### CONCLUDING REMARKS

Turbojet-engine rotor speed and turbine-discharge temperature transients following commands to increase thrust or a simulated afterburner ignition were regulated by proper manipulation of a variable-area exhaust nozzle and engine fuel flow. Closed double-loop controllers using proportional-plus-integral action and noninteraction gain terms corrected

the speed- and temperature-error signals to manipulate the servos. The success of the control configurations depended upon the fast action of the fuel valve and the variable-area exhaust nozzle, in particular, a rapidly opening exhaust nozzle.

Generally, when the over-all transient performance characteristics of the engine were optimized by adjusting the controller settings, it was necessary to compromise the optimum transients that were individually obtained for the controlled parameters. In some cases, the degree of compromise was lessened by using a method of noninteraction to minimize the engine interaction that existed between the control loops.

A control system giving excellent engine transient performance characteristics for both thrust increase and afterburner ignition disturbances is the speed-area, temperature - fuel-flow control configuration with no compensation. With this control, the unfavorable effect of an opening nozzle area on temperature response was hardly discernible, and, consequently, for the chosen operating conditions the speed and temperature responses were mainly a function of their respective controller settings. Simplicity of the control configuration and noncritical adjustment of the speed-area gain setting are definite design advantages that may be realized with this control system.

An alternate control system, which gives acceptable although more oscillatory transient responses, was the speed - fuel-flow, temperature-area control configuration with speed-area compensation. Controller adjustments in both control loops and the noninteraction gain setting were critical for optimum transient performance.

Lewis Flight Propulsion Laboratory  
National Advisory Committee for Aeronautics  
Cleveland, Ohio, October 4, 1957

4476

CF-3 back

## APPENDIX A

## SYMBOLS

$A$	exhaust-nozzle area, sq in.
$f$	frequency, cps
$K$	proportional gain setting
$K_n$	speed-loop controller gain setting
$K_{n/t}$	noninteraction crossover gain term from speed- to temperature-control loops
$K_t$	temperature-loop controller gain setting
$K_{t/n}$	noninteraction crossover gain term from temperature- to speed-control loops
$N$	engine speed, rpm
$N_e$	error between indicated and reference speeds, rpm
$N_i$	indicated rotor speed, rpm
$N_s$	set or reference speed, rpm
$\Delta N_s$	step change in set or reference speed, rpm
$s$	Laplace operator
$T$	engine turbine-discharge temperature, $^{\circ}\text{R}$ or $^{\circ}\text{F}$ , as indicated
$T_e$	error between indicated and reference temperatures, $^{\circ}\text{F}$
$T_i$	indicated turbine-discharge temperature, $^{\circ}\text{F}$
$T_s$	set or reference temperature, $^{\circ}\text{F}$
$\Delta T_s$	step change in set or reference temperature, $^{\circ}\text{F}$
$w_f$	engine fuel flow, lb/hr
$\tau$	controller integrator setting, sec
$\tau_n$	speed-loop controller integrator setting, sec
$\tau_t$	temperature-loop controller integrator setting, sec

## APPENDIX B

SYSTEM RESPONSE EQUATIONS AND STABILITY STUDIES FOR  
DOUBLE-LOOP CONTROLS ON A TURBOJET ENGINE

The block diagram of a double-loop interaction control system with noninteraction gain terms is shown in figure 13. The system to be controlled is represented by the transfer functions  $E_{11}$ ,  $E_{12}$ ,  $E_{21}$ , and  $E_{22}$  blocked together in matrix form with the controlled engine outputs represented by  $C_1$  and  $C_2$  in response to the engine inputs  $M_1$  and  $M_2$ . The controllers are represented by the transfer functions  $G_1$  and  $G_2$ ; the actuating servos by the transfer functions  $S_1$  and  $S_2$ ; and the feedback portions by the transfer functions  $H_1$  and  $H_2$ . The reference inputs to the system are represented by  $R_1$  and  $R_2$ ; a load disturbance in one of the loops is represented by  $D_2$ , which in the case of a turbojet engine may be the action of an afterburner on the effective exhaust-nozzle area. The noninteraction terms between the two control loops are represented by the gains  $K_{21}$  and  $K_{12}$ .

The response equations for this control system in the block diagram are also tabulated in figure 13. The equations are based on the transfer function concept and, therefore, contain frequency-dependent and frequency-independent terms. Transfer-function and steady-state gain values describing the engine, sensors, and servos were determined from frequency and step response data. Gain and dynamic characteristics of the system components are summarized in table I; frequency response data for these components are presented in references 1 and 2.

The system characteristic equation is designated by  $\Delta$  in the table of response equations (fig. 13) and may be equated to zero to define absolute instability of the control system.

For the speed-area, temperature - fuel-flow control system with no compensation, the system characteristics equation reduces to

$$L_1' + L_2' + L_1' L_2' - X'Y' = -1 \quad (B1)$$

where

$$L_1' = G_1 S_1 E_{11} H_1$$

$$L_2' = G_2 S_2 E_{22} H_2$$

$$X' = H_2 G_2 S_2 E_{21}$$

$$Y' = H_1 G_1 S_1 E_{12}$$

and

$S_1 \equiv$  fuel-valve servo

$E_{11} \equiv$  engine temperature response to fuel flow

$H_1 \equiv$  temperature sensor

$S_2 \equiv$  nozzle-area servo

$E_{22} \equiv$  engine speed response to nozzle area

$H_2 \equiv$  speed sensor

$E_{21} \equiv$  engine temperature response to nozzle area

$E_{12} \equiv$  engine speed response to fuel flow

Examination of equation (B1) shows that four terms contribute to the instability of the system. The  $L_1'$  term represents the components in the temperature - fuel-flow loop;  $L_2'$  represents the components in the speed-area control loop; and the  $X'Y'$  path includes the engine interaction terms between the two loops and all the components in the system outside the engine.

An experimental study was made on this control configuration to determine the system instability characteristics as a function of controller settings. The system oscillation frequencies for various combinations of controller gain settings were determined experimentally and were correlated with frequency response data to solve for the  $L_1'$ ,  $L_2'$ , and  $X'Y'$  terms in the system characteristic equation.

Figure 14 is a vector representation of the basic speed-area, temperature - fuel-flow control system characteristic equation at instability for two combinations of controller gains. In the top part of figure 14 the system was operated at a high temperature controller gain  $K_t$  and a low speed controller gain  $K_n$  and shows the  $L_1'$  term in equation (B1) or the temperature - fuel-flow control loop to have the greatest contribution to the -1 instability vector; the magnitude of the  $X'Y'$  term was insignificant. The bottom part of figure 14 shows the effect of lowering  $K_t$  and increasing  $K_n$ ; the temperature - fuel-flow control loop still remains the predominating control loop driving the system

toward instability. Comparing the vectors in both parts indicates that the setting of the temperature - fuel-flow controller gain is critical; variation of the speed-area controller gain has little effect in causing system instability. The magnitude and phase of the vectors are within experimental accuracy.

A similar experimental instability study was made with the speed - fuel-flow, temperature-area control configuration with speed-area compensation. Verification of the experimental instability points with this control configuration was not as precise as with the previous control system because the instability oscillation frequencies were high, and the open-loop frequency data were not as well defined in these regions. The vector diagrams for this control system (fig. 14(b)), however, show the critical control paths.

Solving the system characteristic equation for the speed - fuel-flow, temperature-area control configuration with speed-area compensation gives

$$L_1'' + L_2'' + L_1''L_2'' - X''Y'' + Z'' = -1 \quad (B2)$$

where

$$L_1'' = G_1 S_1 E_{11} H_1$$

$$L_2'' = G_2 S_2 E_{22} H_2$$

$$X'' = H_2 G_2 S_2 E_{21}$$

$$Y'' = H_1 G_1 S_1 E_{12}$$

$$Z'' = G_1 K_{12} S_2 E_{21} H_1$$

and

$S_1 \equiv$  fuel-valve servo

$E_{11} \equiv$  engine speed response to fuel flow

$H_1 \equiv$  speed sensor

$S_2 \equiv$  nozzle-area servo

$E_{22} \equiv$  engine temperature response to nozzle area

$H_2 \equiv$  temperature sensor

$E_{21} \equiv$  engine speed response to nozzle area

$E_{12} \equiv$  engine temperature response to fuel flow

$K_{12} \equiv$  noninteraction gain term

Equation (B2) shows that five terms contribute to the instability of the system. The  $L_1''$  term represents the components in the speed - fuel-flow control loop;  $L_2''$  represents the components in the temperature - exhaust-nozzle-area control loop;  $X''Y''$  represents the components in the speed-area and temperature - fuel-flow control loops; and  $Z''$  represents the components in the noninteraction gain, speed-area control loop.

Figure 14(b) is a vector representation of the characteristic equation for this control system at instability for two combinations of controller gain settings. The two  $K_t$  gain settings were chosen from the high and low values in the overshoot and settle-out time curves in figures 8(c) and (d). The critical path for both conditions is through the noninteraction crossover, engine speed-area term, speed sensor, and the speed - fuel-flow loop controller. Gain settings of the noninteraction crossover are critical for stabilizing the basic speed - fuel-flow, temperature-area control system.

#### REFERENCES

1. Wenzel, L. M., Hart, C. E., and Craig, R. T.: Experimental Comparison of Speed - Fuel-Flow and Speed-Area Controls on a Turbojet Engine for Small Step Disturbances. NACA TN 3926, 1957.
2. Hart, C. E., Wenzel, L. M., and Craig, R. T.: Experimental Investigation of Temperature Feedback Control Systems Applicable to Turbojet-Engine Control. NACA TN 3936, 1957.
3. Otto, Edward W., Gold, Harold, and Hiller, Kirby W.: Design and Performance of Throttle-Type Fuel Controls for Engine Dynamic Studies. NACA TN 3445, 1955.
4. Boksenbom, Aaron S., and Hood, Richard: General Algebraic Method Applied to Control Analysis of Complex Engine Types. NACA Rep. 980, 1950. (Supersedes NACA TN 1908.)
5. Phillips, W. E., Jr.: An Analysis of Controlled Interacting Systems. M.S. Thesis, Case Inst. Tech., 1954.

TABLE I. - ENGINE, SENSOR, AND CONTROLLER DYNAMICS

System Component	Gain and Dynamic Characteristics (a)	
Engine		
$N/w_f$ , rpm/(lb/hr)	$0.403 \left( \frac{1}{1 + 0.83s} \right) e^{-0.083s}$	
$N/A$ , rpm/sq in.	$18.7 \left( \frac{1}{1 + 0.83s} \right) e^{-0.021s}$	
$T/w_f$ , °F/(lb/hr)	$0.115 \left( \frac{1 + 1.3 \times 0.83s}{1 + 0.83s} \right) e^{-0.079s}$	
$T/A$ , °F/sq in.	$-2.13 \left( \frac{1 + 0.4 \times 0.83s}{1 + 0.83s} \right) e^{-0.020s}$	
Fuel distribution <sup>b</sup>	Amplitude ratio	Phase shift, deg
Frequency, cps		
2.45	0.518	-41.4
2.20	0.533	-43.4
6.16	0.53	-28
6.34	0.53	-24
Sensors		
Temperature (thermo-couples and amplifier), volt/°F	$0.023 \left( \frac{1}{1 + 0.3s} \right)$	
Speed, volt/rpm	$1.83 \times 10^{-3}$	
Servos		
Fuel valve	309 (lb/hr)/volt; amplitude ratio, flat to approx. 10 cps; dead time of valve position to input signal, 0.005 sec	
Nozzle area	5.08 sq in./volt; for dynamic characteristics see response data in fig. 1	
Controller		
Proportional-plus-integral	$K \left( 1 + \frac{1}{\tau s} \right)$	

<sup>a</sup>The characteristics for describing the engine and the sensors are for engine operation in the region defined by speed and temperature values between points A and B on fig. 3.

<sup>b</sup>The dynamics contributed by the fuel distribution system are given in refs. 1 and 2. The frequencies presented here are those of interest in appendix B.

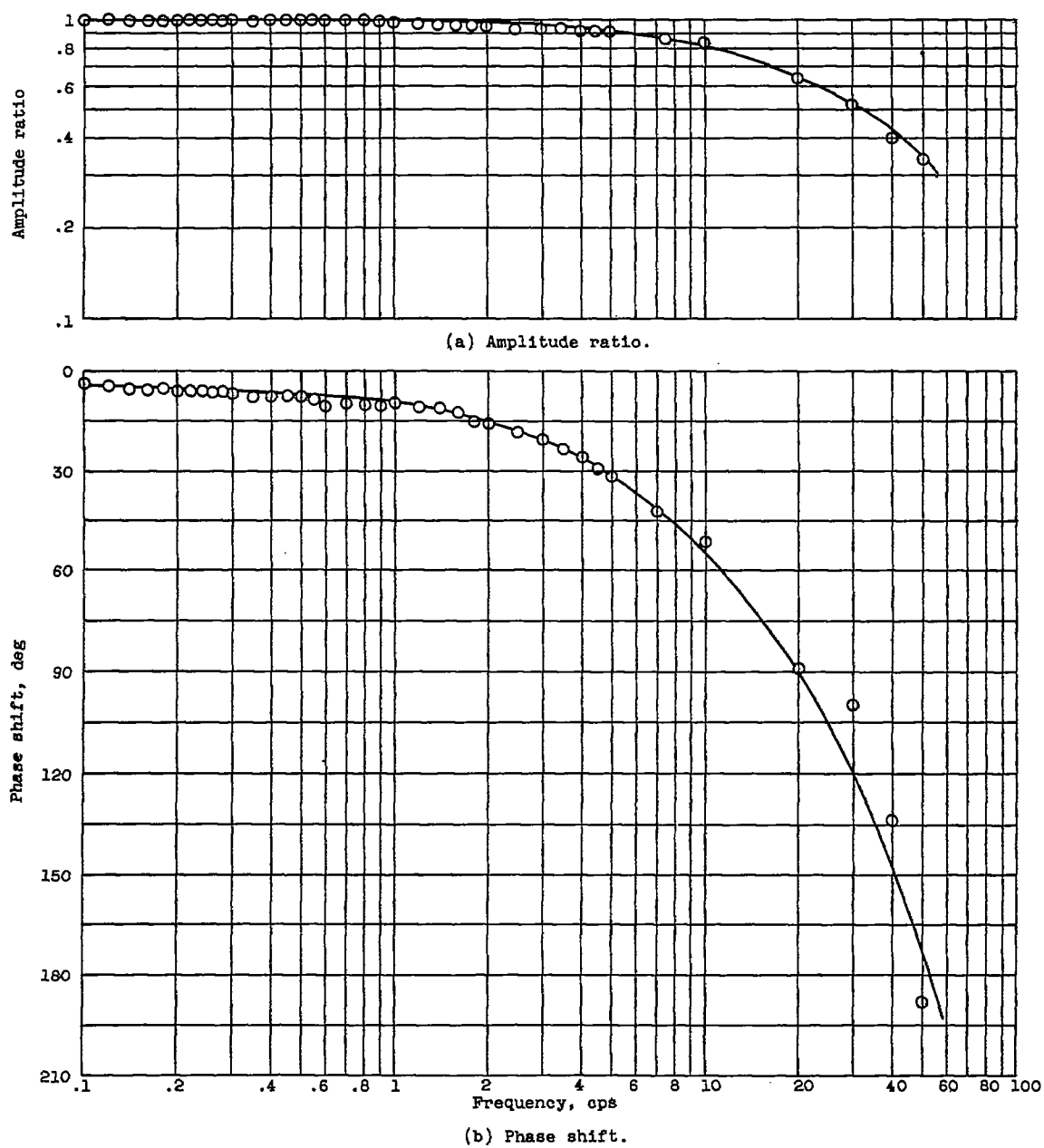
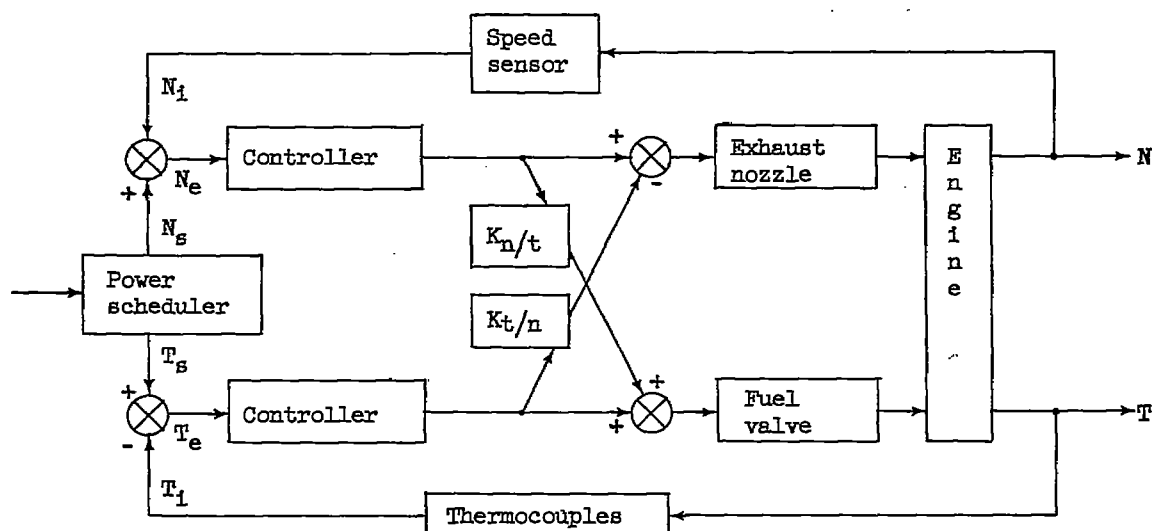
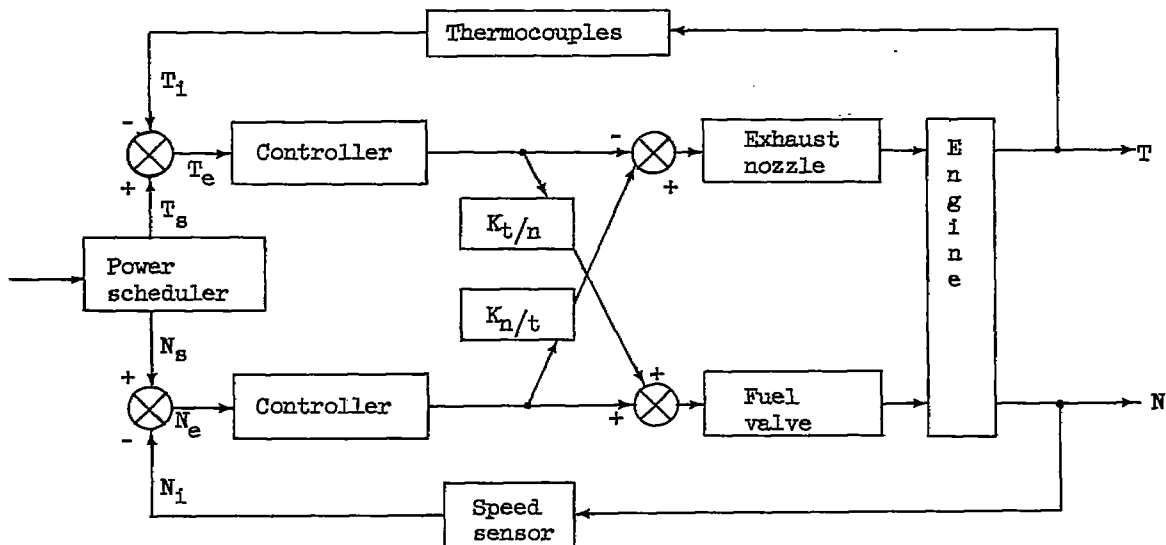


Figure 1. - Frequency response of exhaust-nozzle position to sinusoidal input of  $\pm 5.0$  percent of rated area (ref. 1).



(a) Speed-area, temperature - fuel-flow control systems.



(b) Speed - fuel-flow, temperature-area control systems.

Figure 2. - Block diagrams of the various control system configurations.

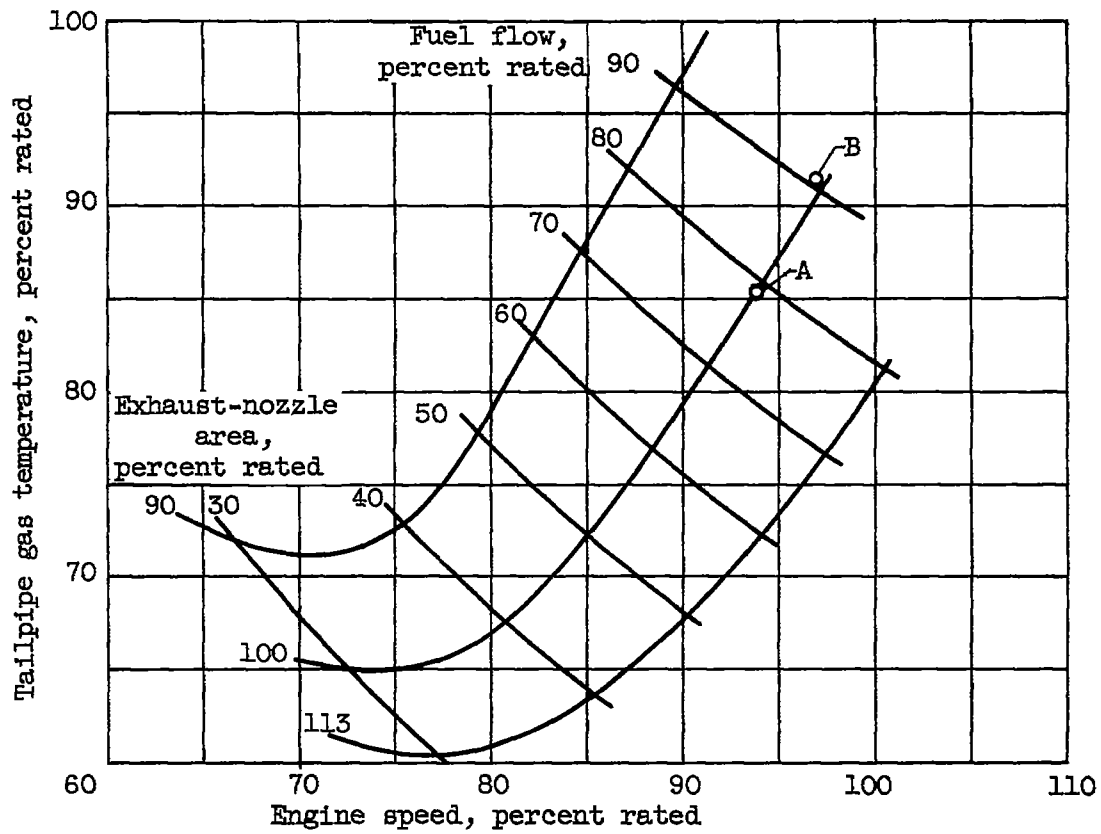
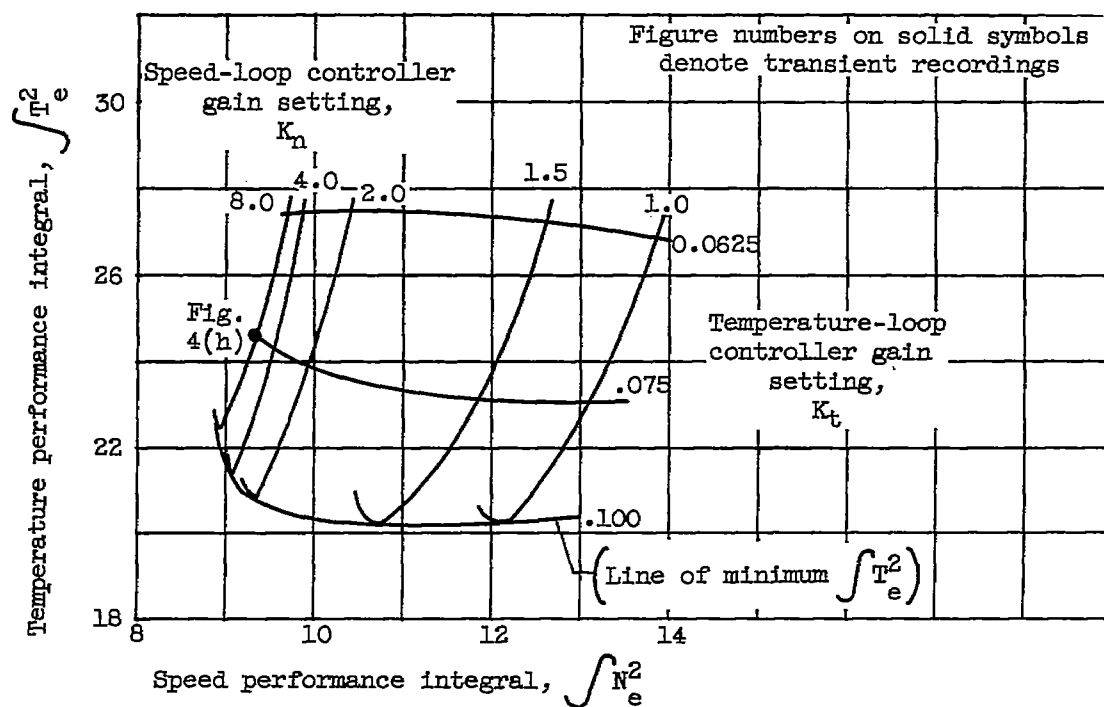
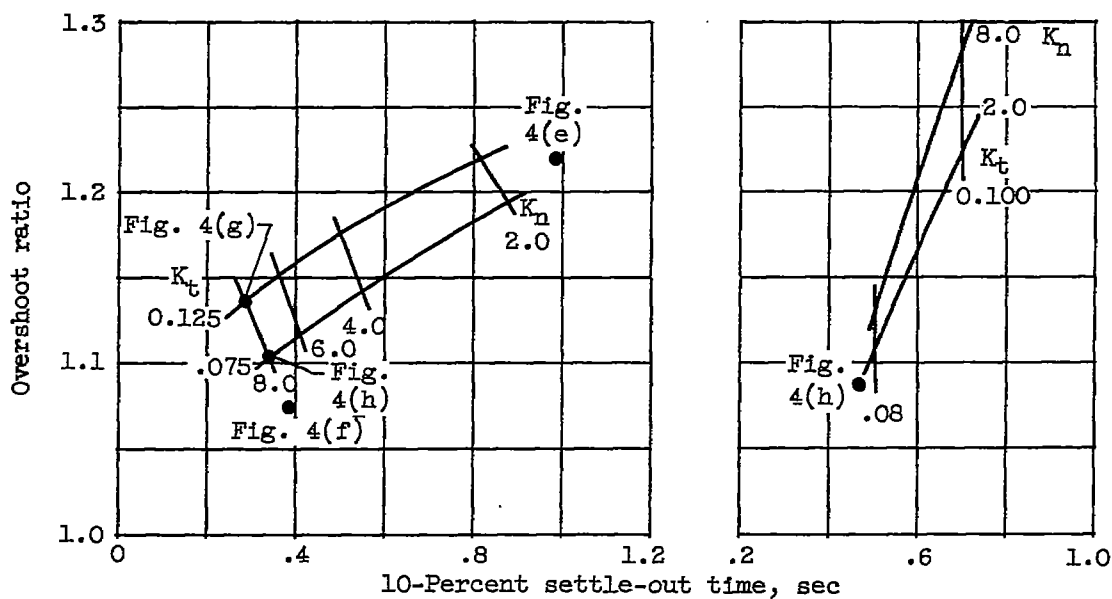


Figure 3. - Engine steady-state operating map.



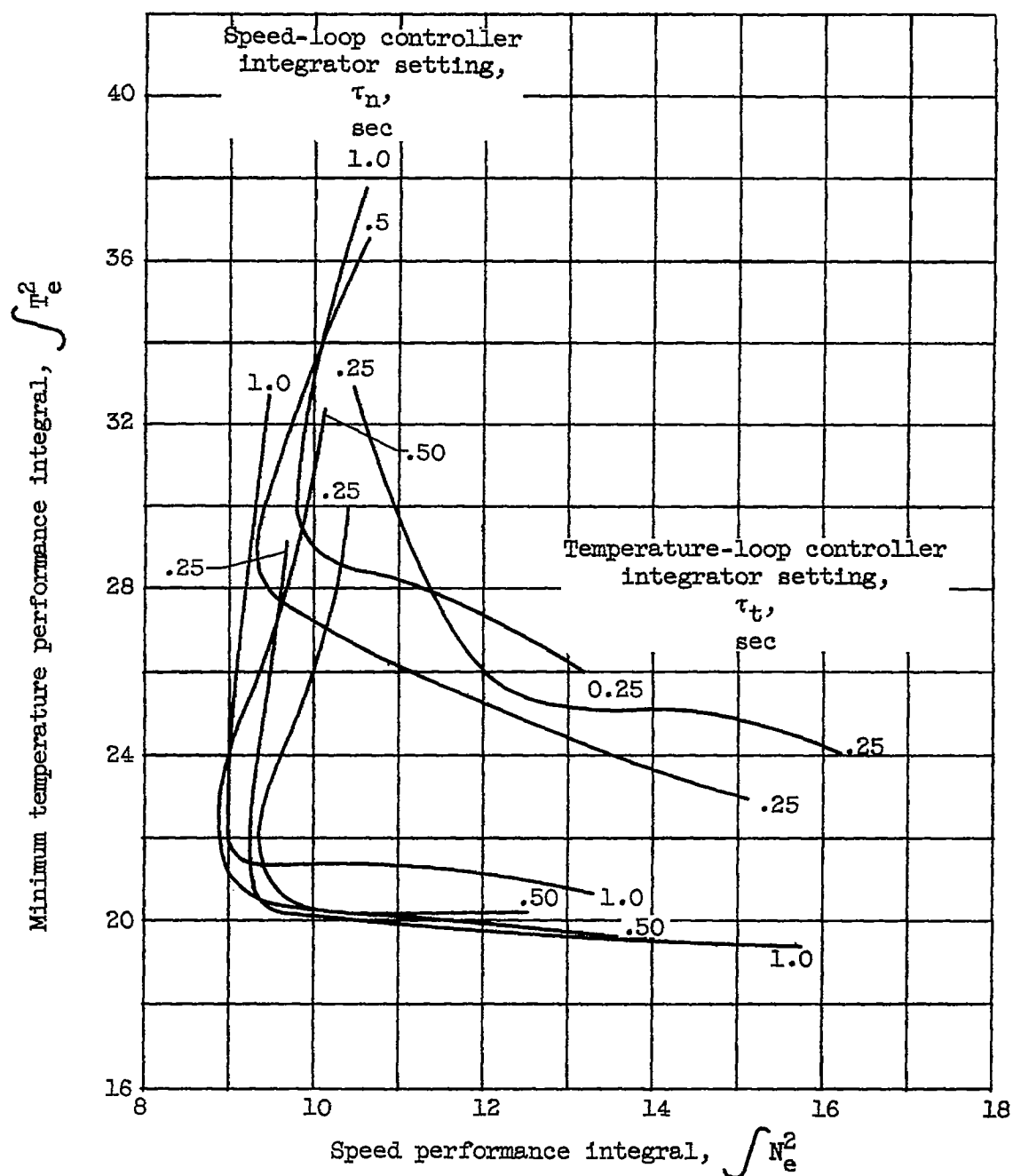
(a) Integral performance.



(b) Speed transient analysis.

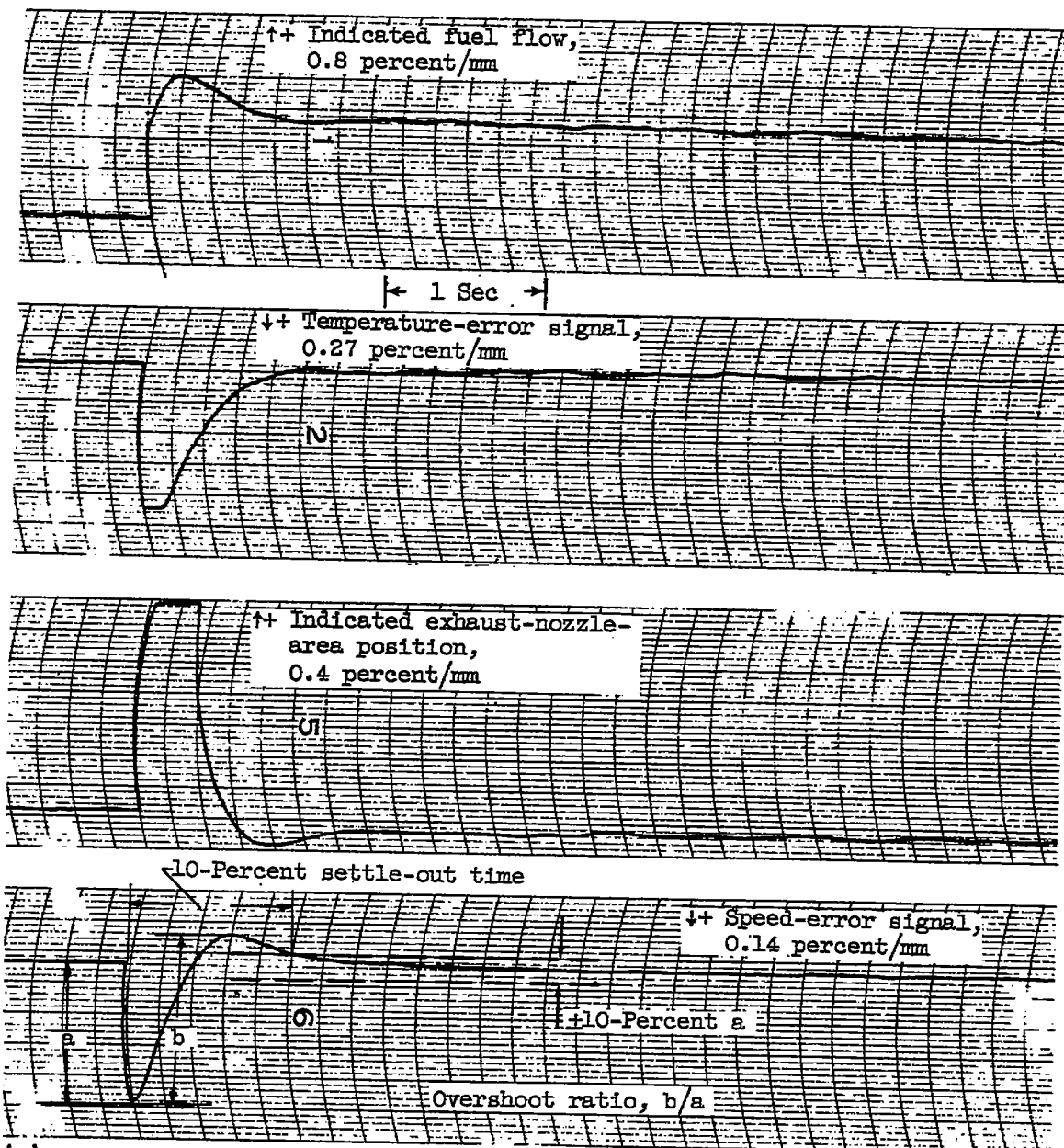
(c) Temperature transient analysis.

Figure 4. - Speed-area, temperature - fuel-flow control system with no compensation. Speed- and temperature-loop controller integrator settings, 0.5 second.



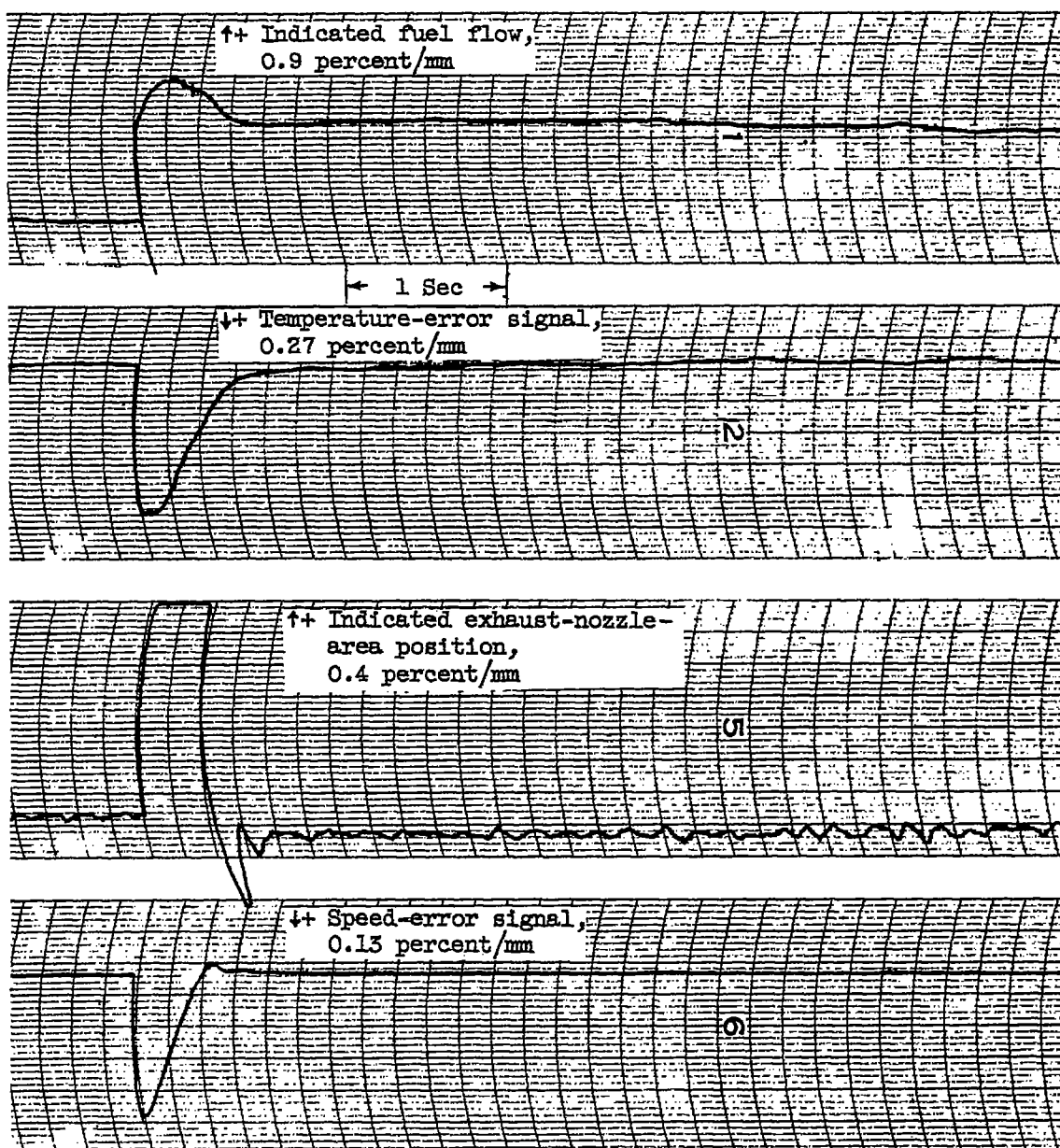
(d) Minimum performance integrals for each combination of controller integrator.

Figure 4. - Continued. Speed-area, temperature - fuel-flow control system with no compensation. Speed- and temperature-loop controller integrator settings, 0.5 second.



(e) Transient data. Speed-loop controller gain setting, 2.0; temperature-loop controller gain setting, 0.05.

Figure 4. - Continued. Speed-area, temperature - fuel-flow control system with no compensation. Speed- and temperature-loop controller integrator settings, 0.5 second.

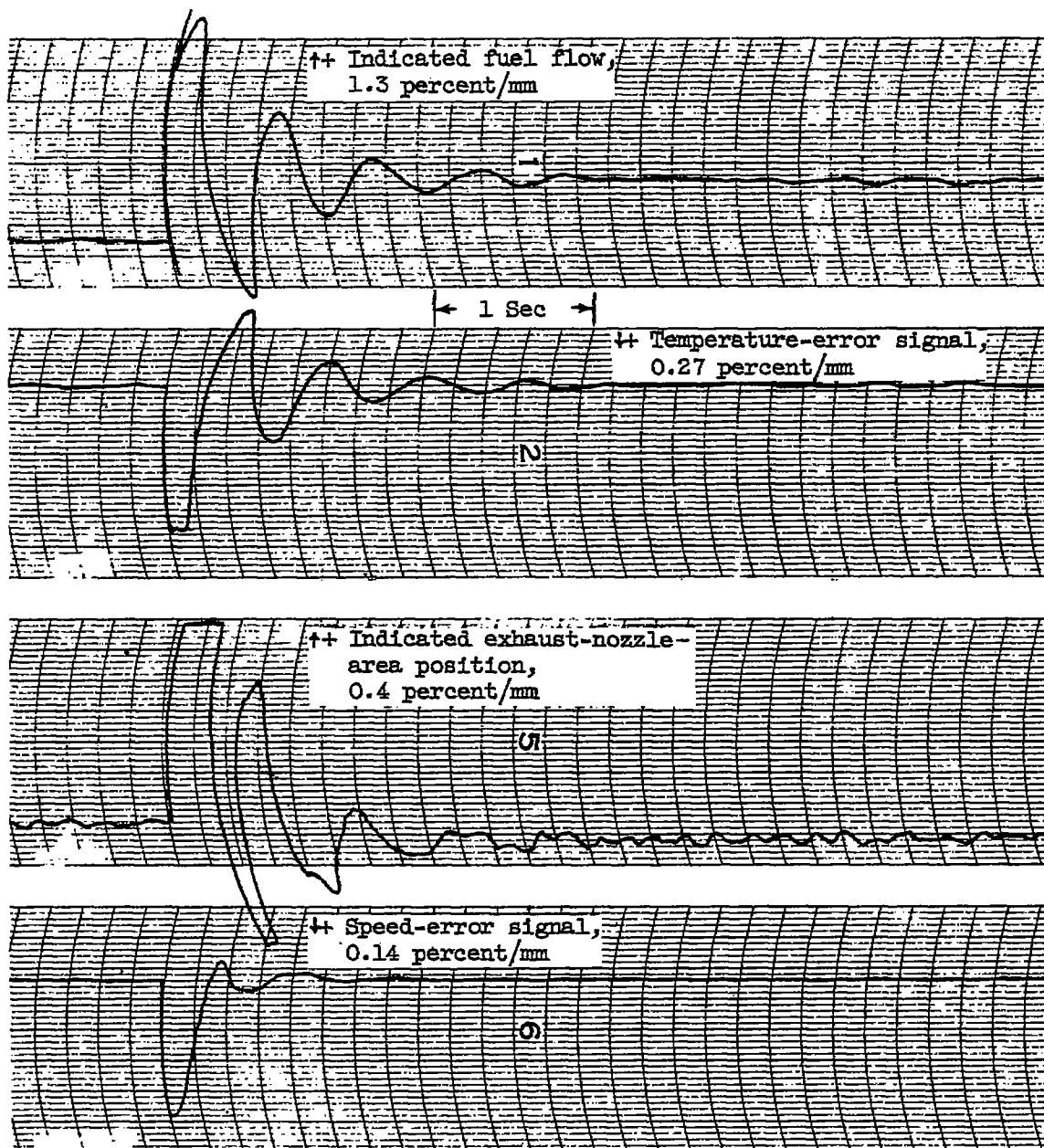


(f) Transient data. Speed-loop controller gain setting, 8.0; temperature-loop controller gain setting, 0.05.

Figure 4. - Continued. Speed-area, temperature - fuel-flow control system with no compensation. Speed- and temperature-loop controller integrator settings, 0.5 second.

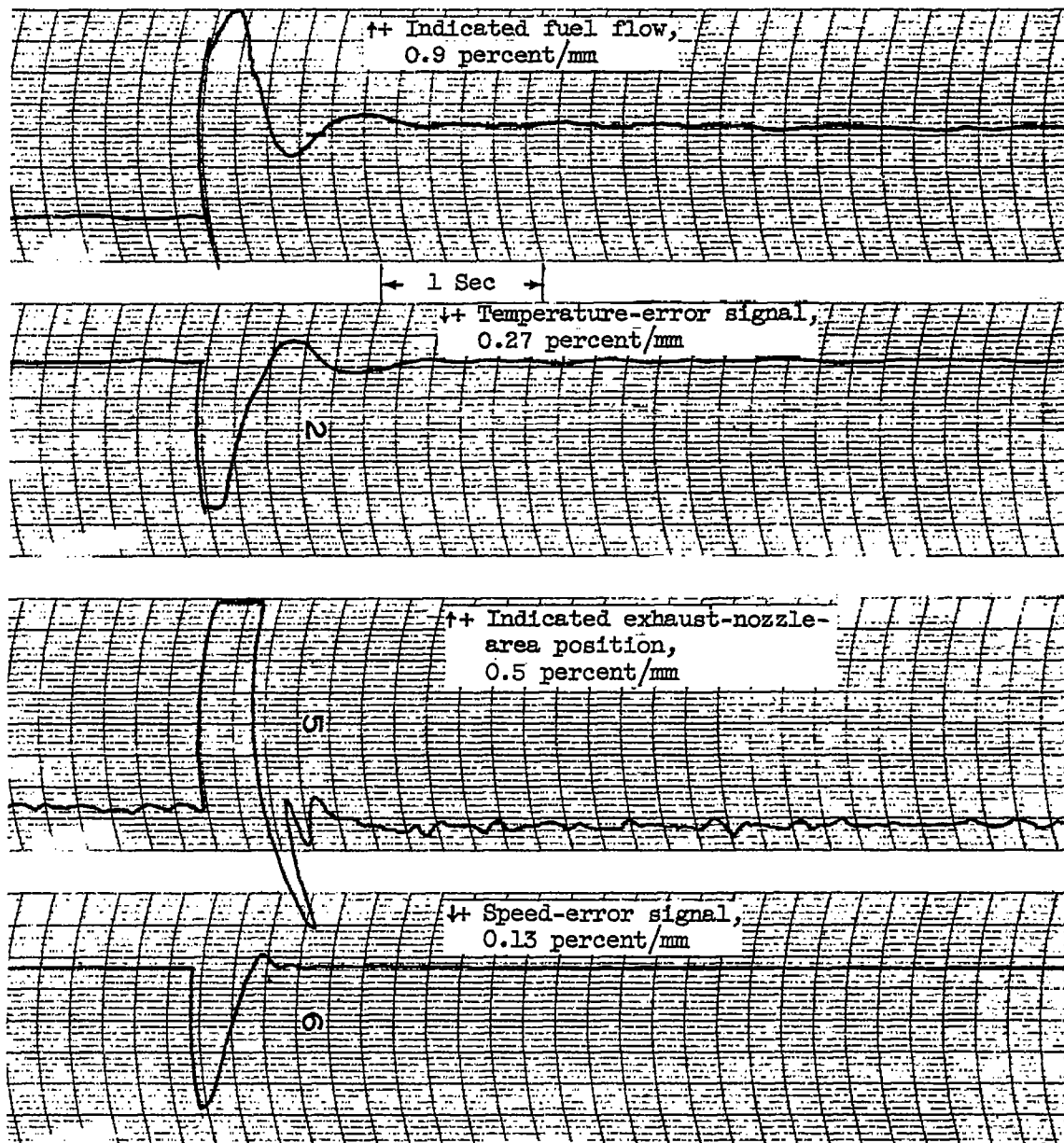
4476

CF-5



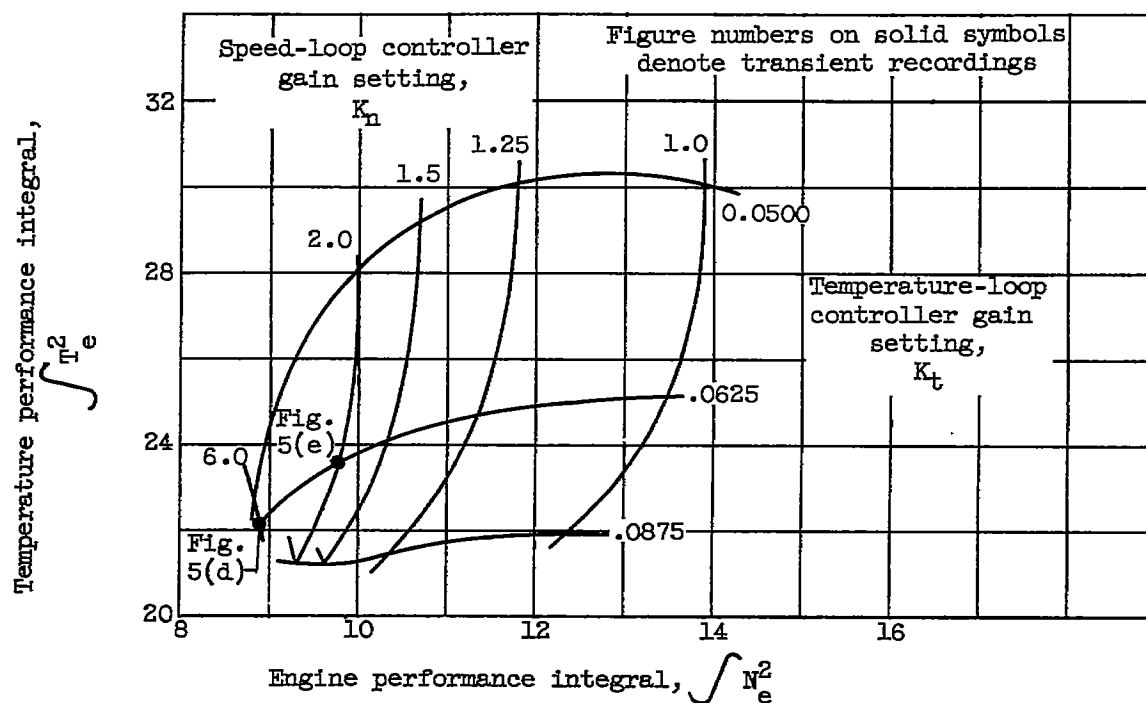
(g) Transient data. Speed-loop controller gain setting, 8.0; temperature-loop controller gain setting, 0.125.

Figure 4. - Continued. Speed-area, temperature - fuel-flow control system with no compensation. Speed- and temperature-loop controller integrator settings, 0.5 second.

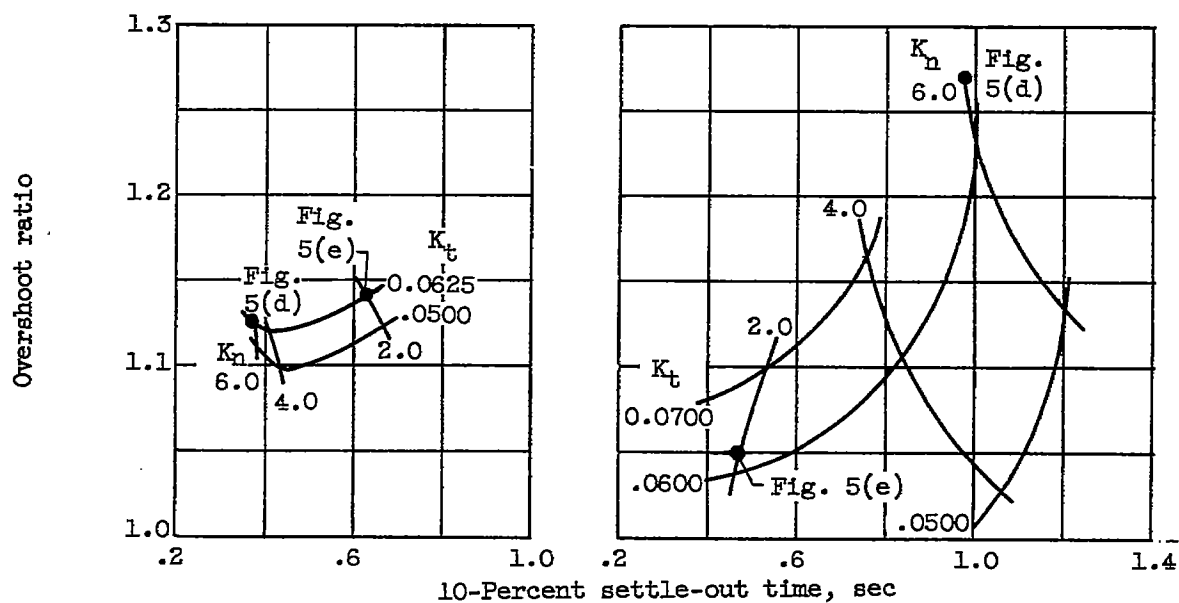


(h) Transient data. Speed-loop controller gain setting, 8.0; temperature-loop controller gain setting, 0.075.

Figure 4. - Concluded. Speed-area, temperature - fuel-flow control system with no compensation. Speed- and temperature-loop controller integrator settings, 0.5 second.



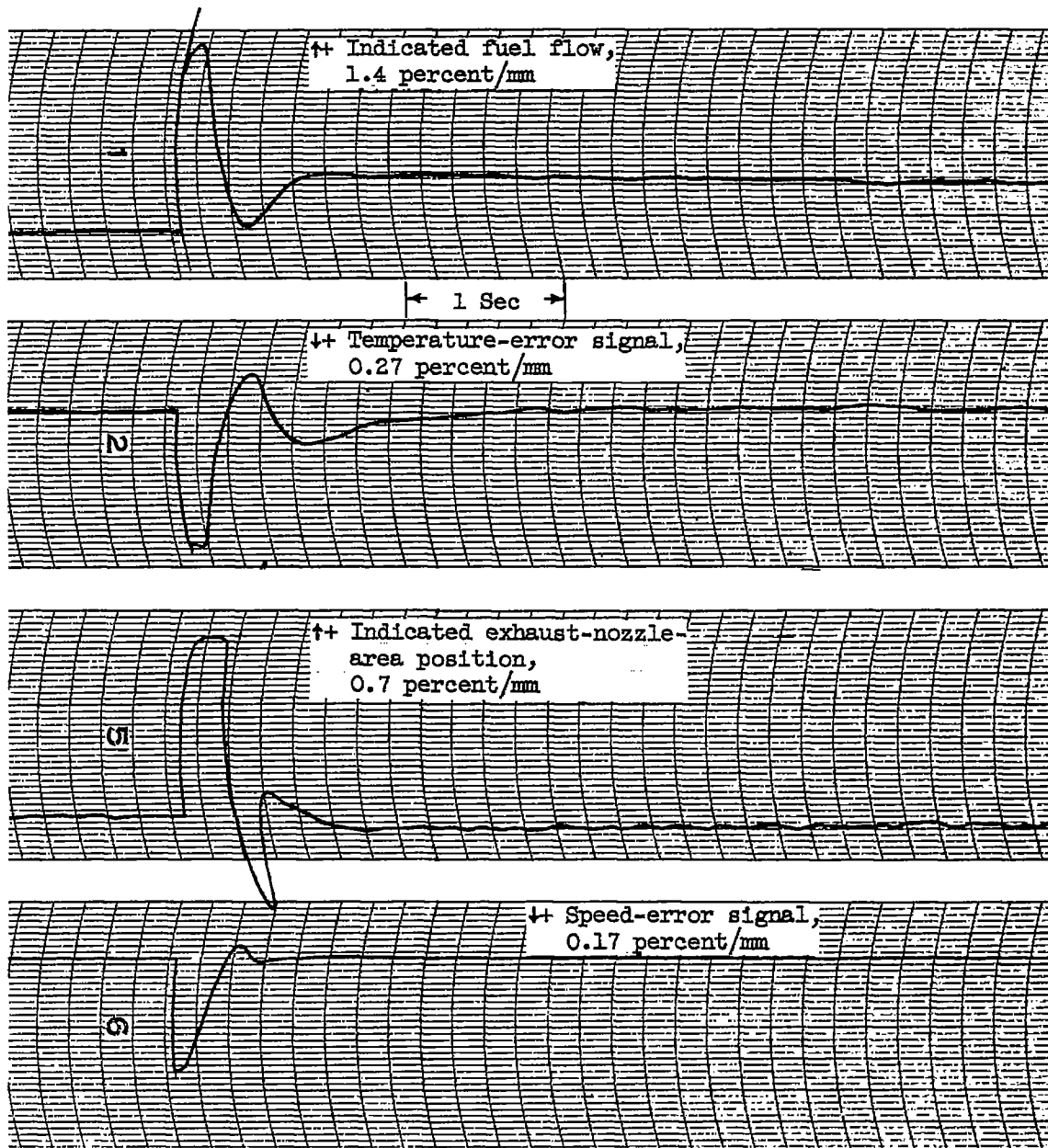
(a) Integral performance.



(b) Speed transient analysis.

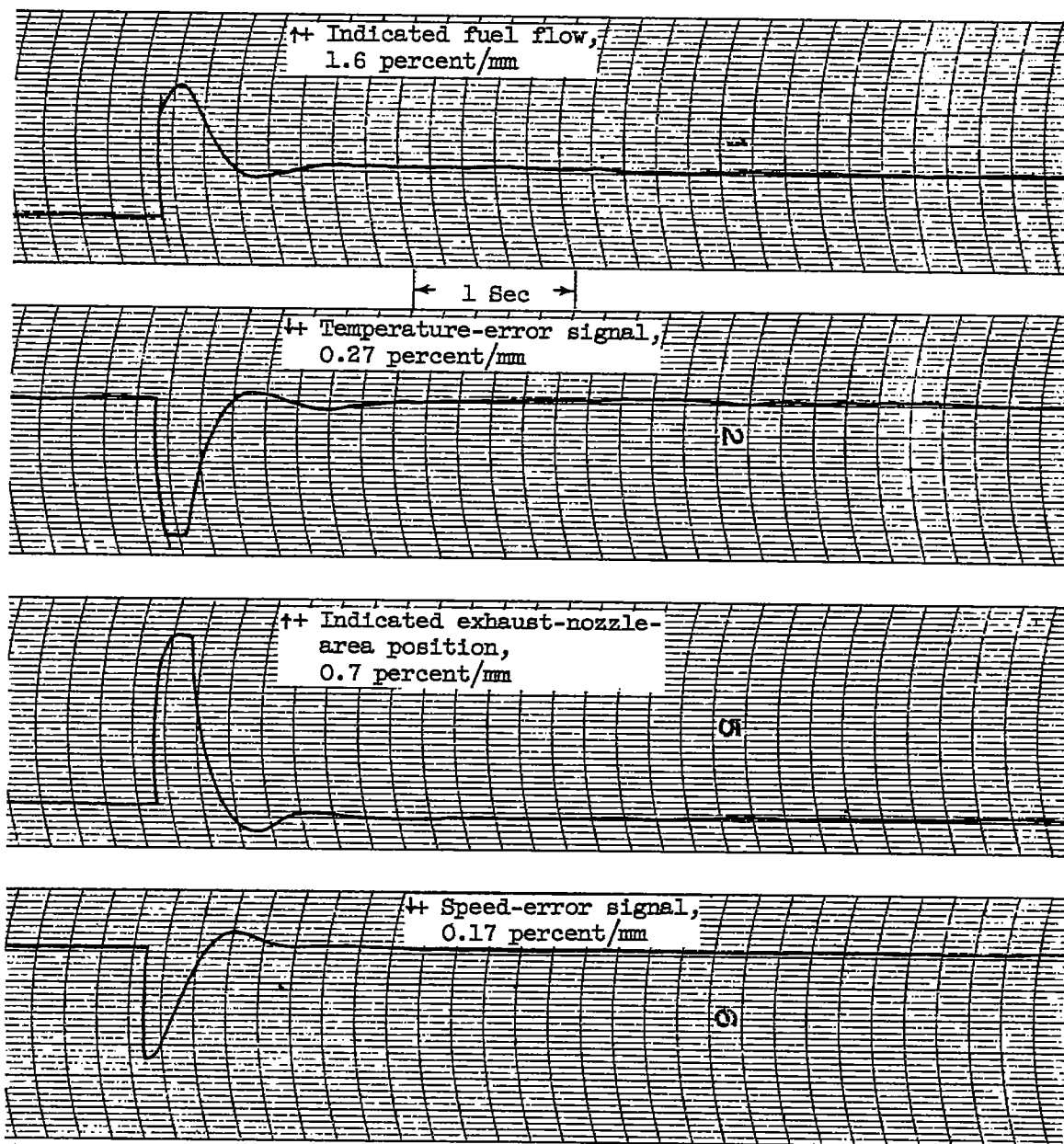
(c) Temperature transient analysis.

Figure 5. - Speed-area, temperature - fuel-flow control system with speed - fuel-flow compensation. Speed- and temperature-loop controller integrator settings, 0.5 second.



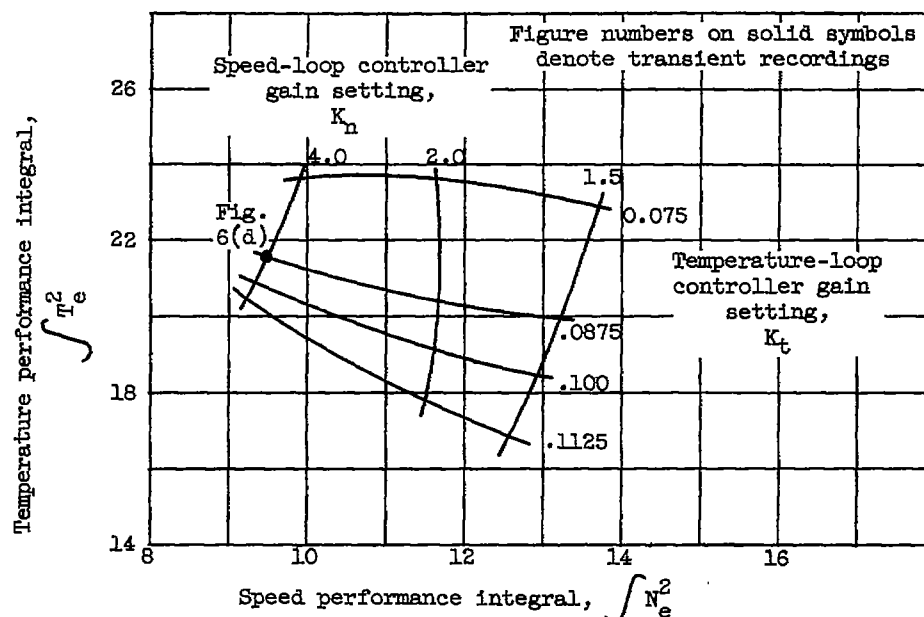
(d) Transient data. Speed-loop controller gain setting, 6.0; temperature-loop controller gain setting, 0.0625.

Figure 5. - Continued. Speed-area, temperature - fuel-flow control system with speed - fuel-flow compensation. Speed- and temperature-loop controller integrator settings, 0.5 second.

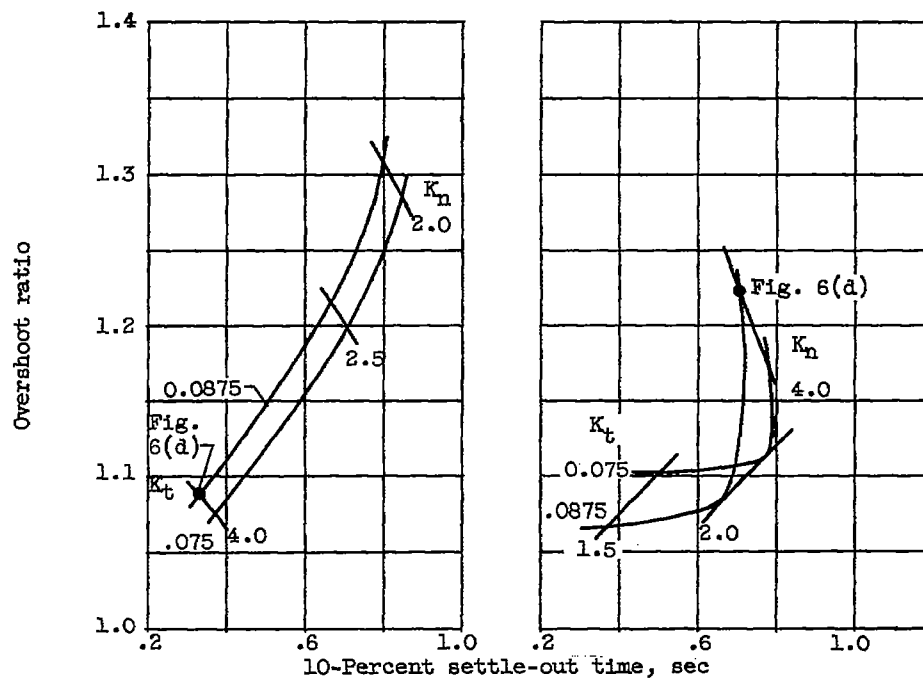


(e) Transient data. Speed-loop controller gain setting, 2.0; temperature-loop controller gain setting, 0.625.

Figure 5. - Concluded. Speed-area, temperature - fuel-flow control system with speed - fuel-flow compensation. Speed- and temperature-loop controller integrator settings, 0.5 second.



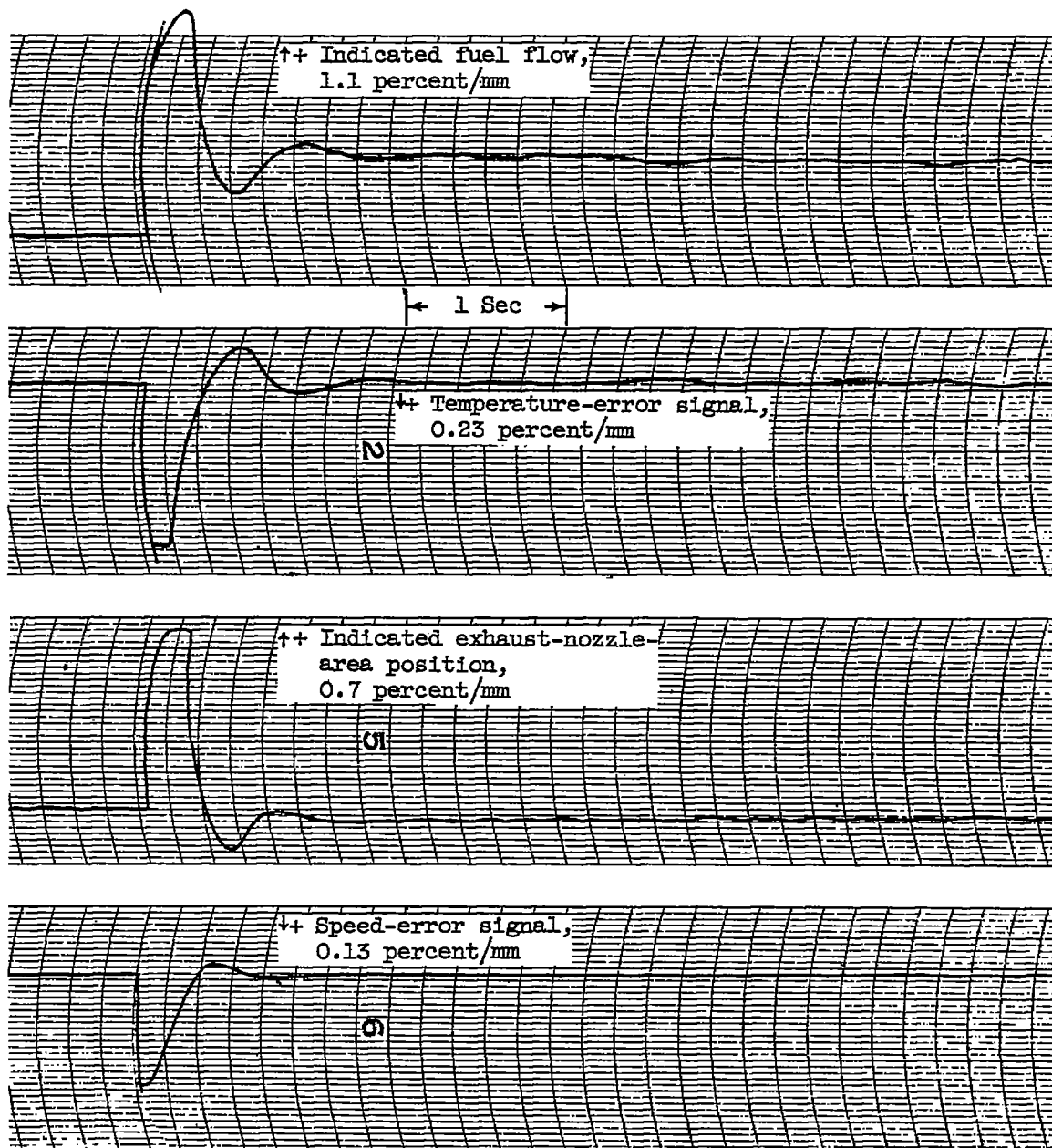
(a) Integral performance.



(b) Speed transient analysis.

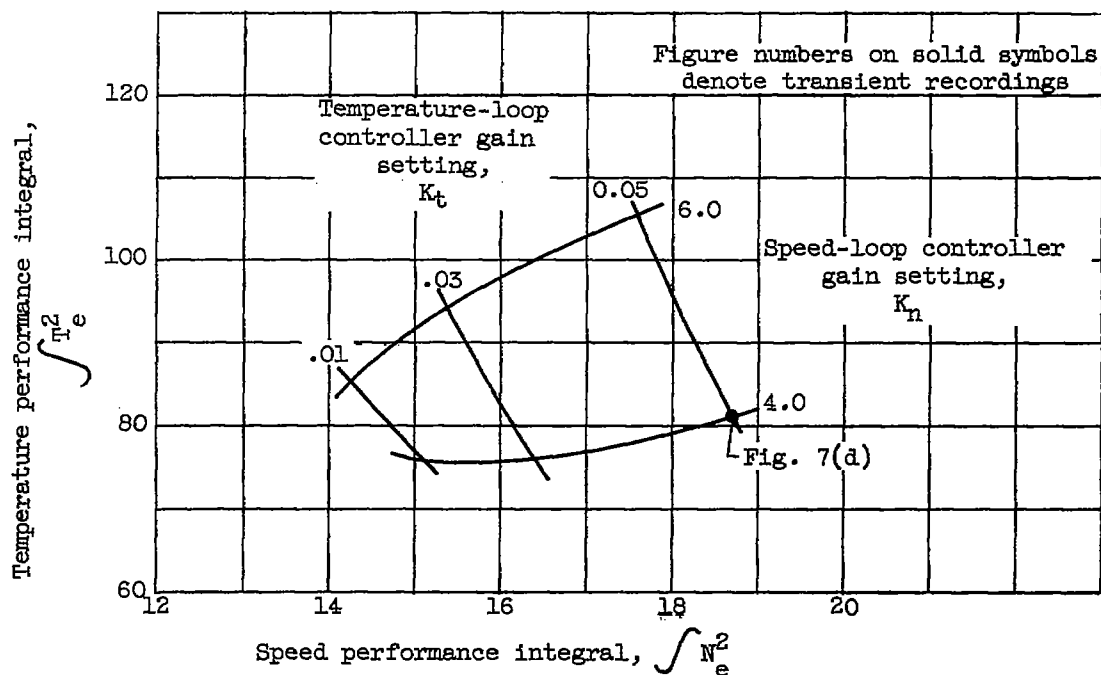
(c) Temperature transient analysis.

Figure 6. - Speed-area, temperature - fuel-flow control system with temperature-area compensation. Speed-loop controller integrator setting, 0.25 second; temperature-loop controller integrator setting, 0.05 second.

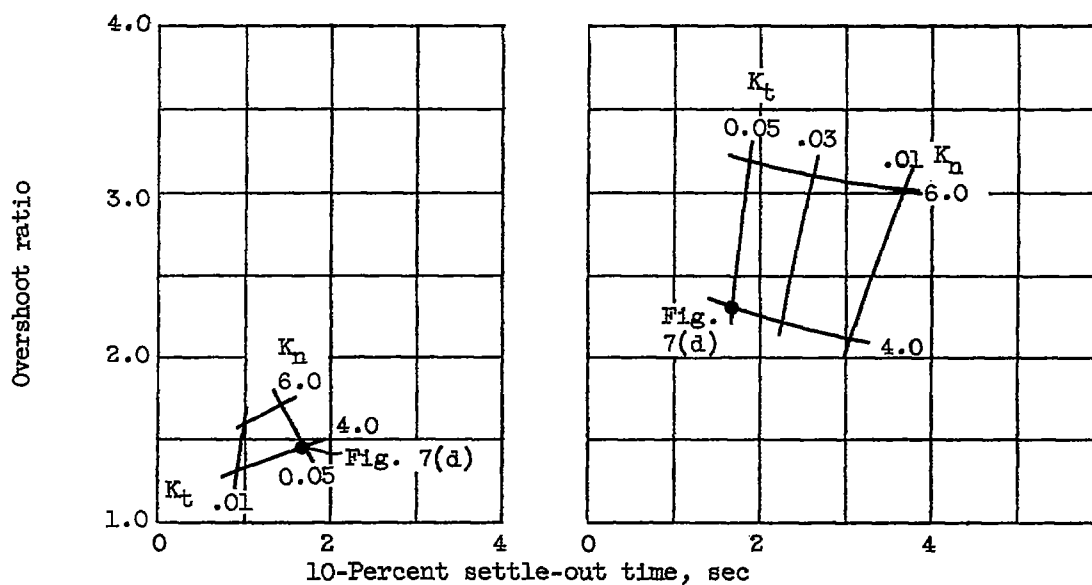


(d) Transient data. Speed-loop controller gain setting, 4.0; temperature-loop controller gain setting, 0.0875.

Figure 6. - Concluded. Speed-area, temperature - fuel-flow control system with temperature-area compensation. Speed-loop controller integrator setting, 0.25 second; temperature-loop controller integrator setting, 0.05 second.



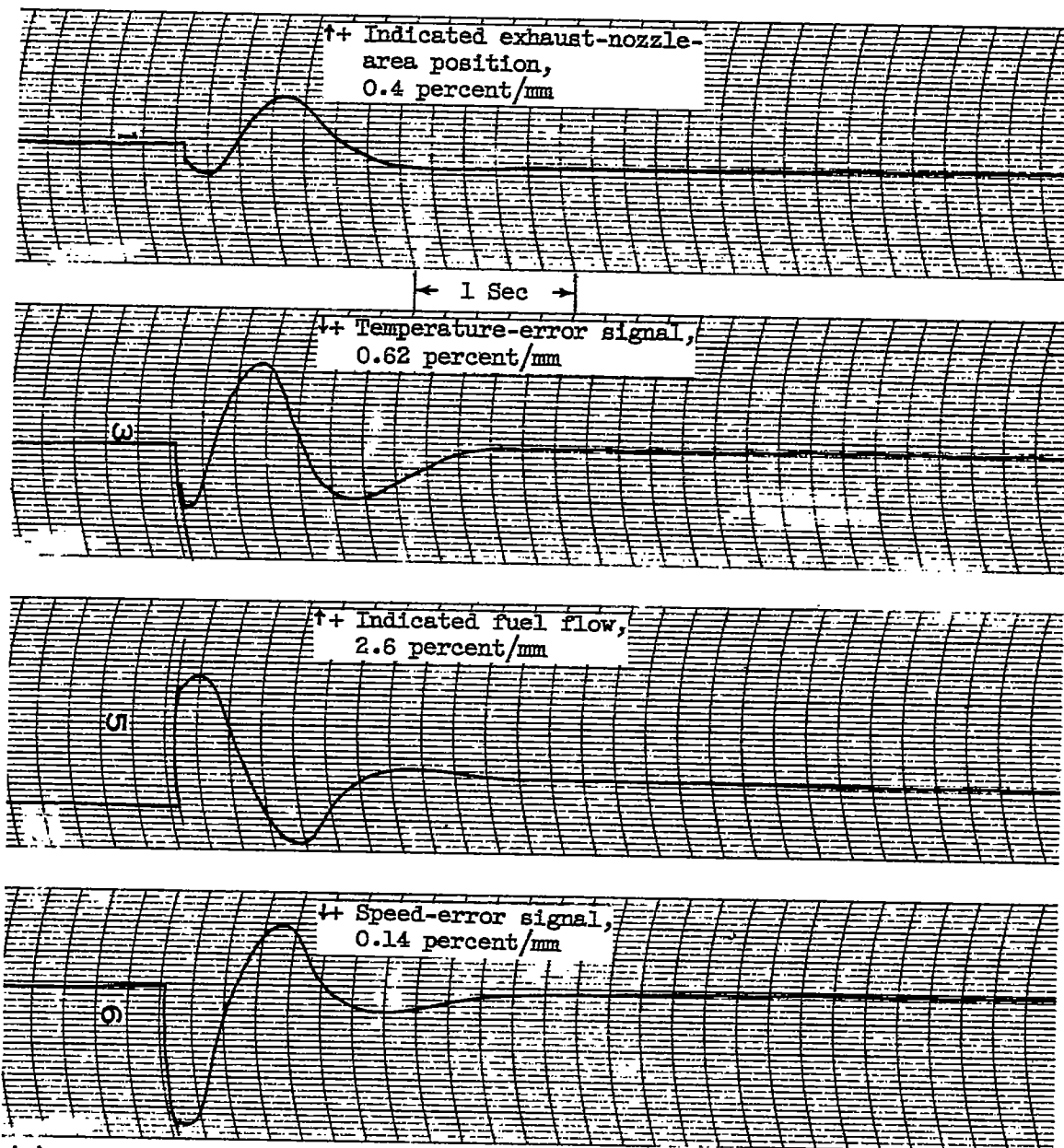
(a) Integral performance.



(b) Speed transient analysis.

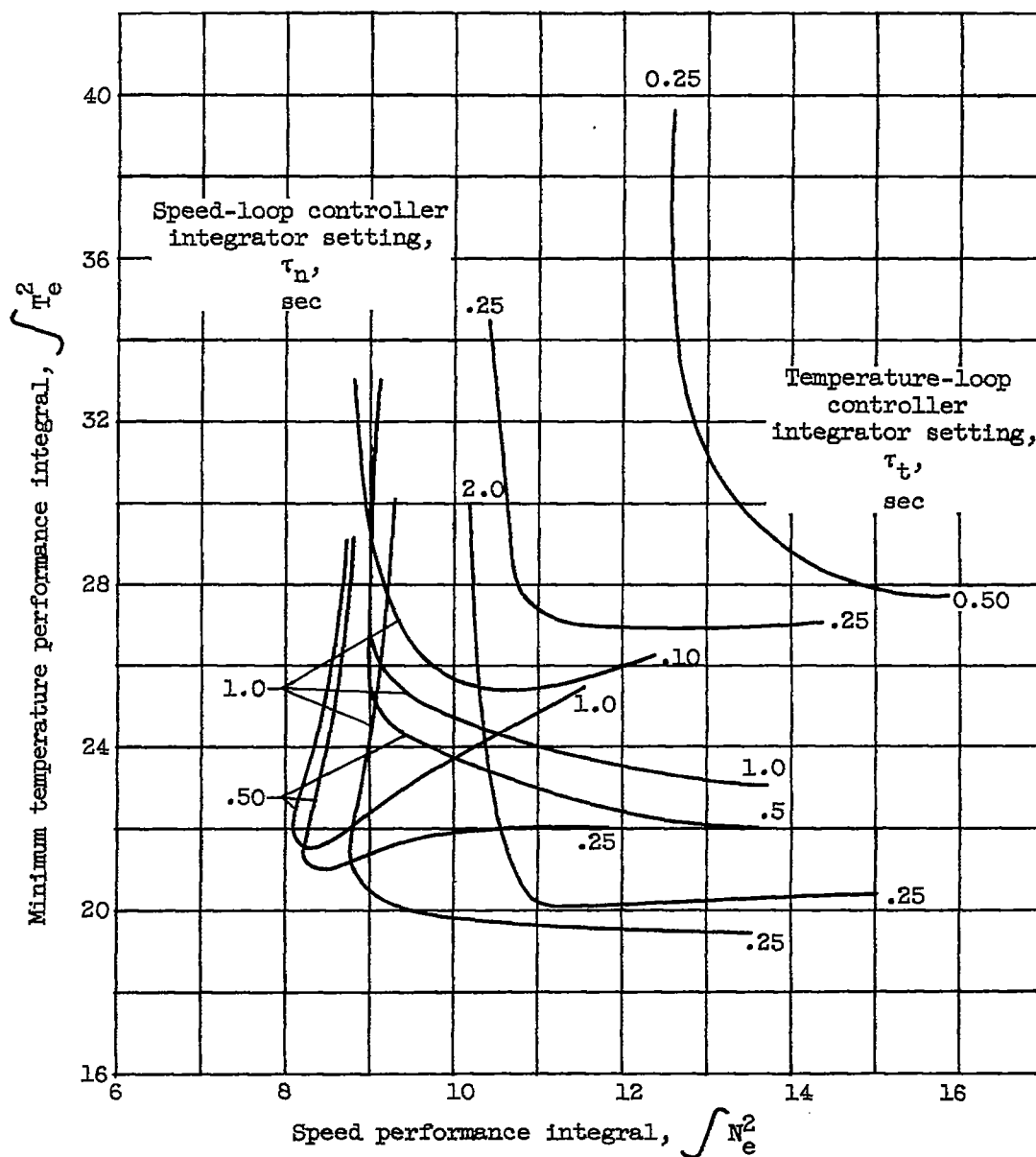
(c) Temperature transient analysis.

Figure 7. - Speed - fuel-flow, temperature-area control system with no compensation. Speed-loop controller integrator setting, 1.0 second; temperature-loop controller integrator setting, 0.25 second.



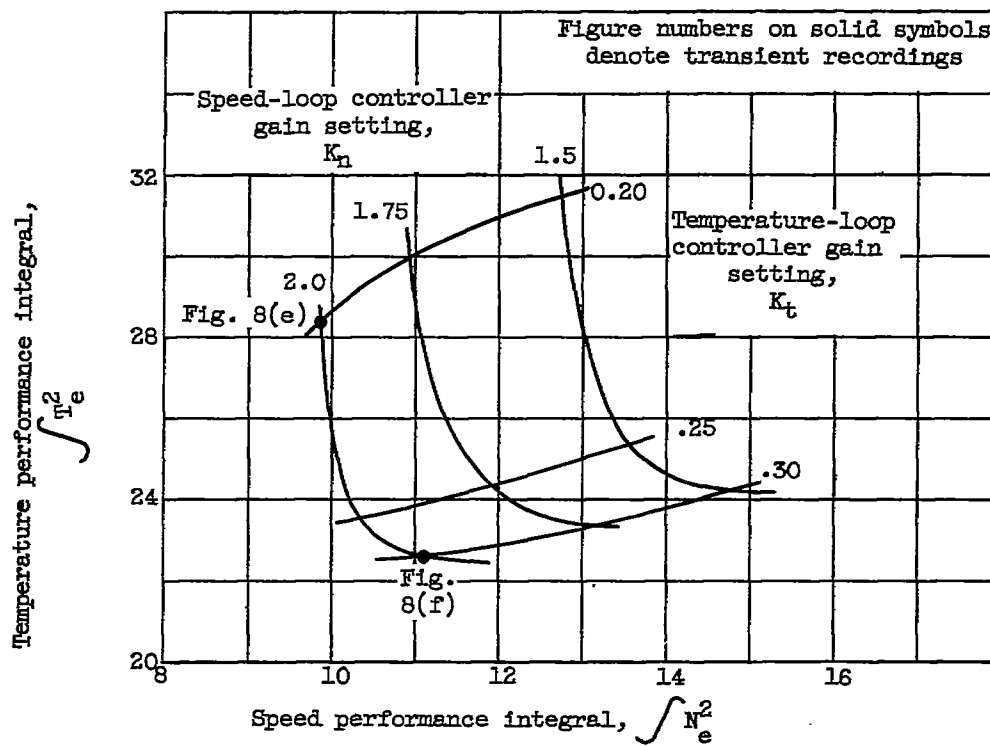
(d) Transient data. Speed-loop controller gain setting, 4.0; temperature-loop controller gain setting, 0.05.

Figure 7. - Concluded. Speed - fuel-flow, temperature-area control system with no compensation. Speed-loop controller integrator setting, 1.0 second; temperature-loop controller integrator setting, 0.25 second.

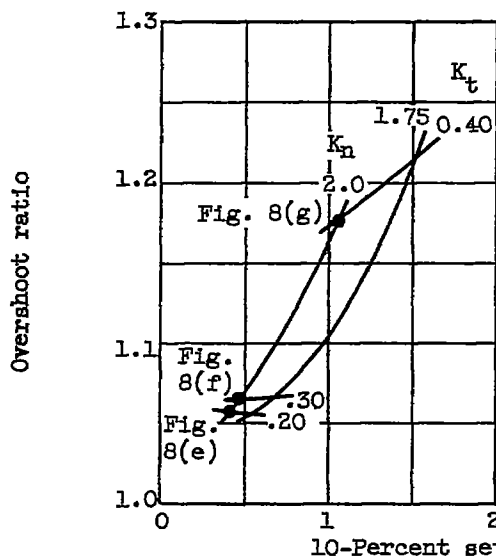


(a) Minimum integrals for each controller time constant combination.

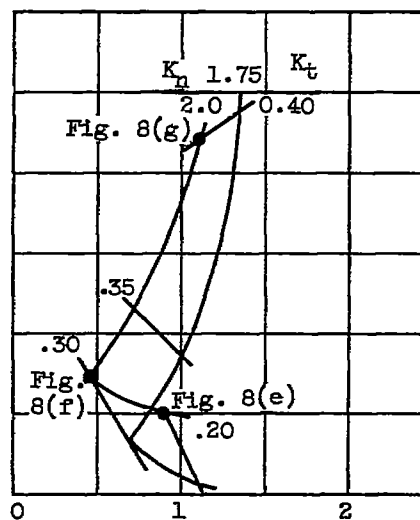
Figure 8. - Speed - fuel-flow, temperature-area control system with speed-area compensation. Speed-loop controller integrator setting, 0.5 second; temperature-loop controller integrator setting, 0.25 second.



(b) Integral performance.

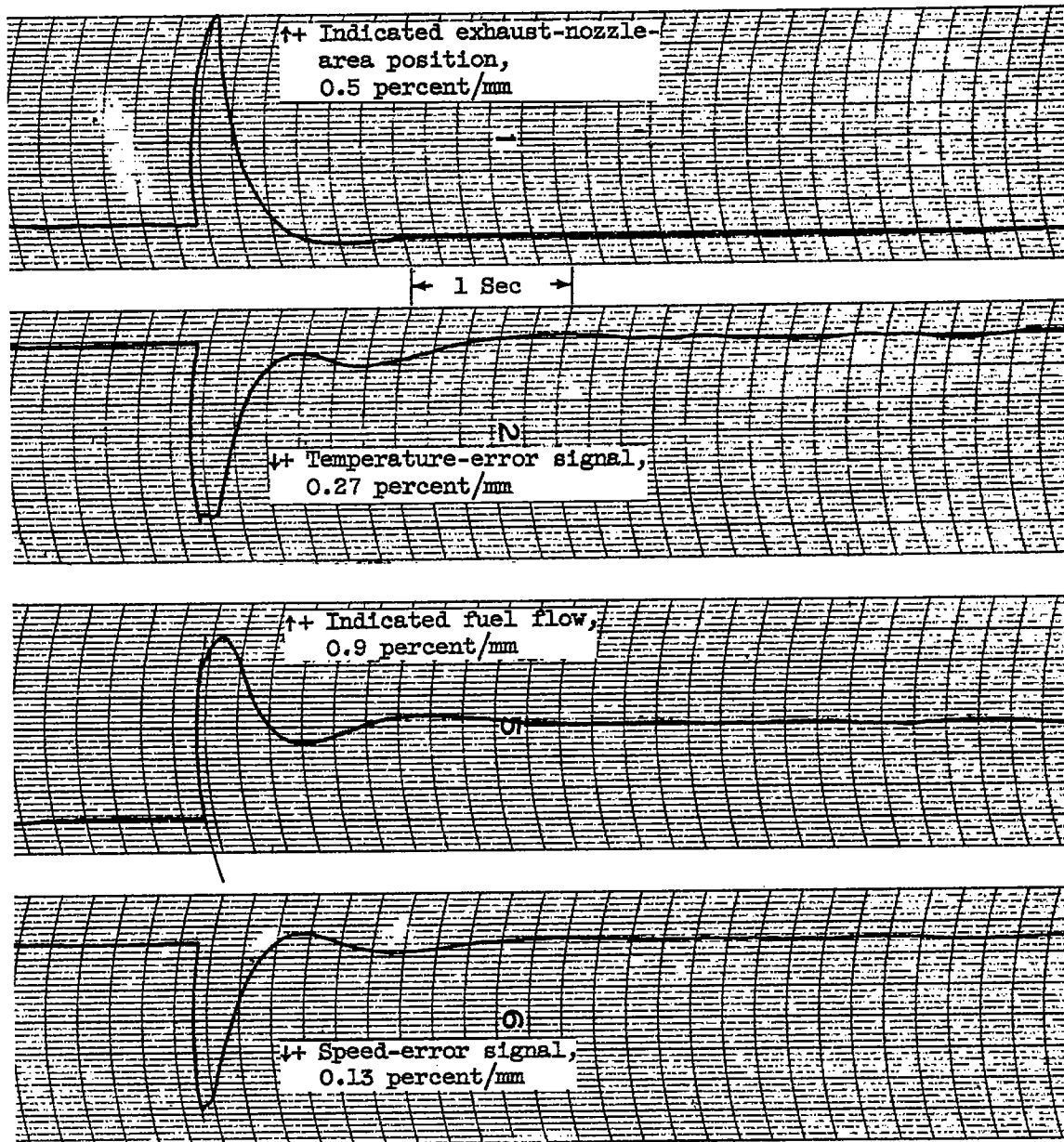


(c) Speed transient analysis.



(d) Temperature transient analysis.

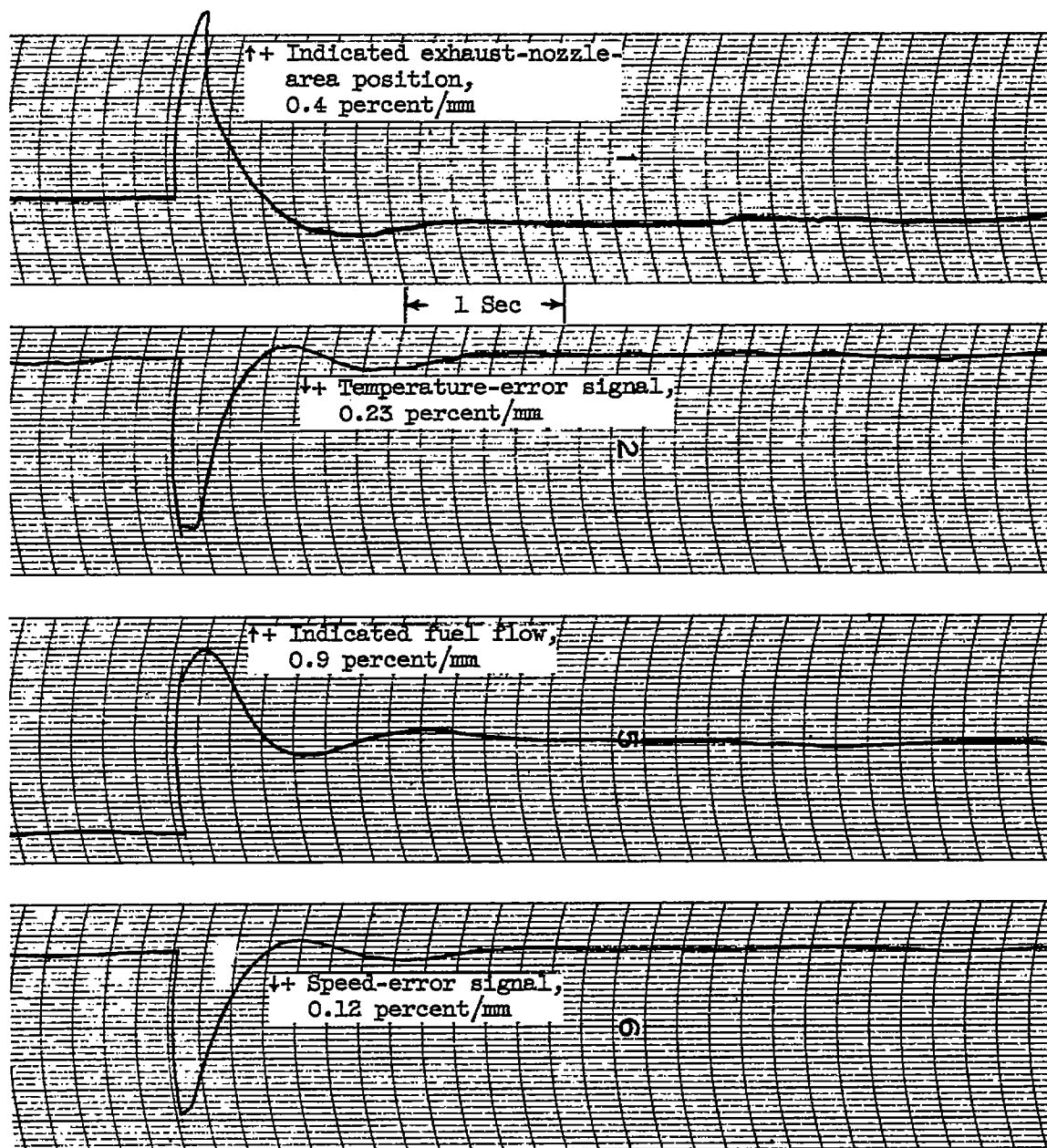
Figure 8. - Continued. Speed - fuel-flow, temperature-area control system with speed-area compensation. Speed-loop controller integrator setting, 0.5 second; temperature-loop controller integrator setting, 0.25 second.



(e) Transient data. Speed-loop controller gain setting, 2.0; temperature-loop controller gain setting, 0.20.

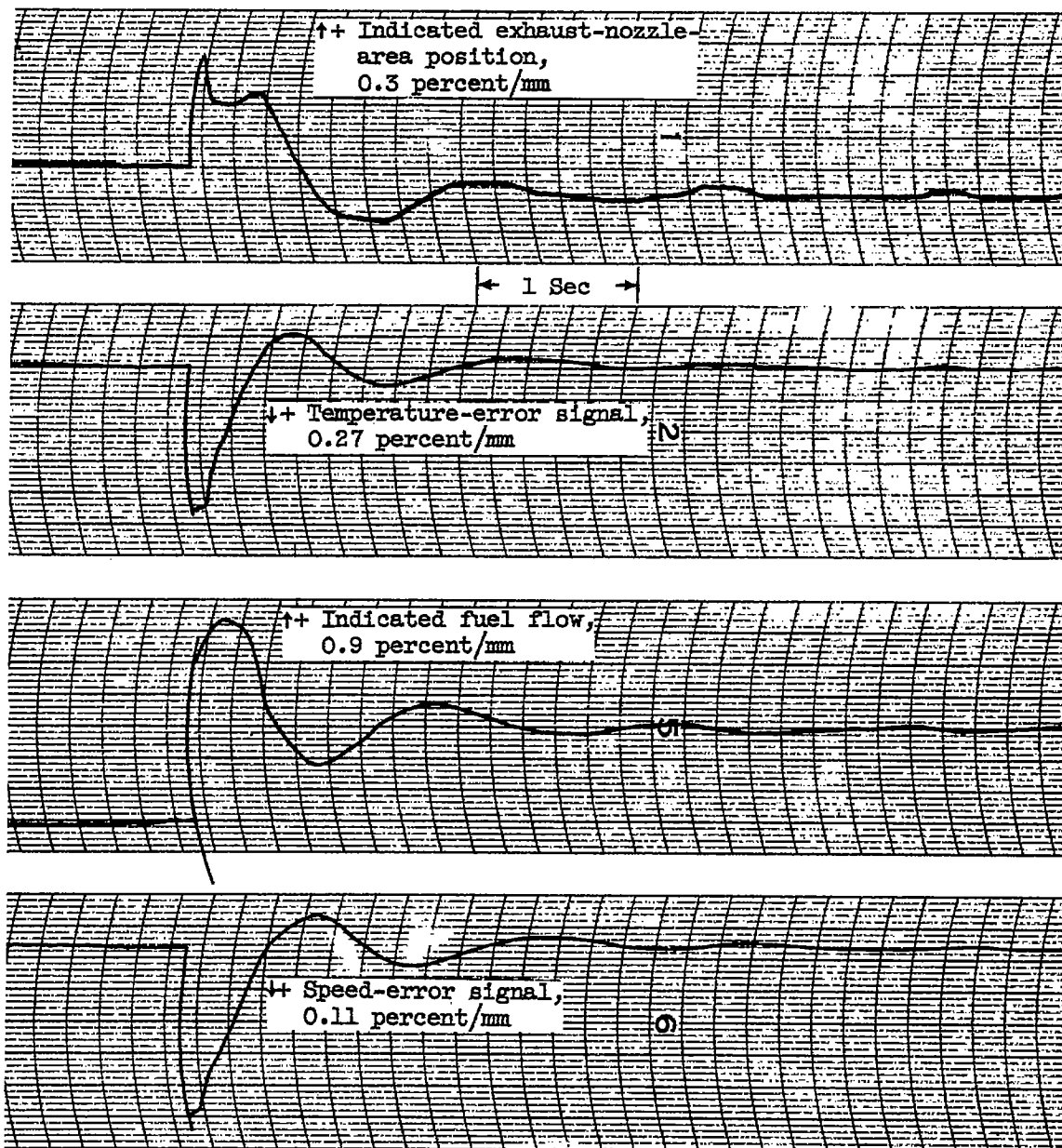
Figure 8. - Continued. Speed - fuel-flow, temperature-area control system with speed-area compensation. Speed-loop controller integrator setting, 0.5 second; temperature-loop controller integrator setting, 0.25 second.

4476



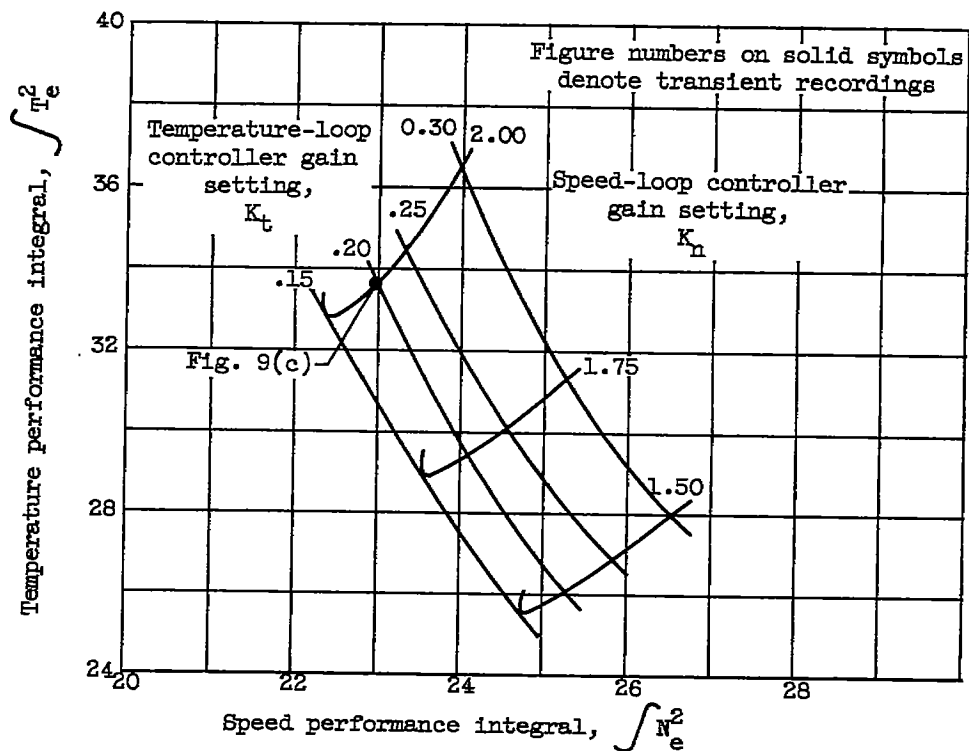
(f) Transient data. Speed-loop controller gain setting, 2.0; temperature-loop controller gain setting, 0.30.

Figure 8. - Continued. Speed - fuel-flow, temperature-area control system with speed-area compensation. Speed-loop controller integrator setting, 0.5 second; temperature-loop controller integrator setting, 0.25 second.

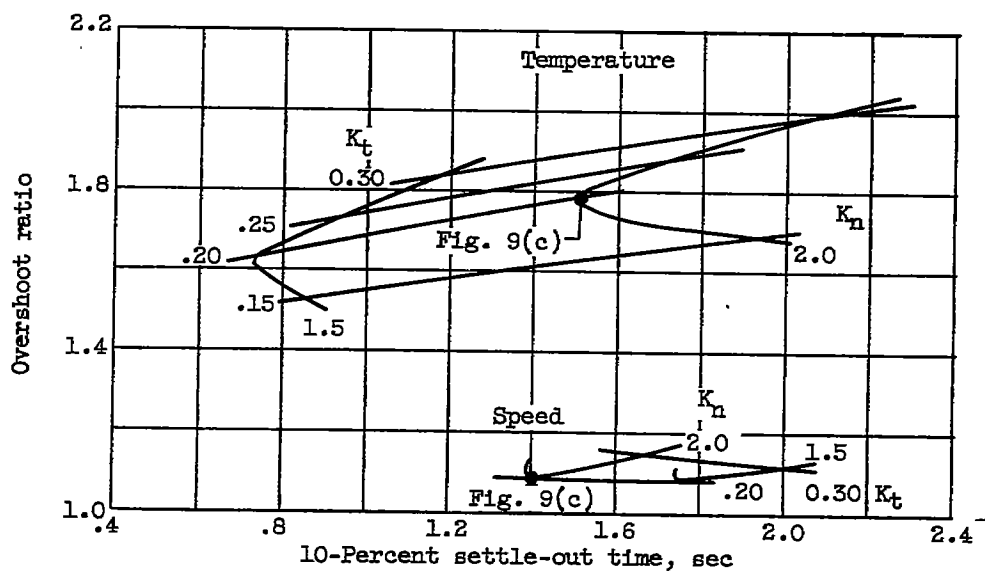


(g) Transient data. Speed-loop controller gain setting, 2.0; temperature-loop controller gain setting, 0.40.

Figure 8. - Concluded. Speed - fuel-flow, temperature-area control system with speed-area compensation. Speed-loop controller integrator setting, 0.5 second; temperature-loop controller integrator setting, 0.25 second.

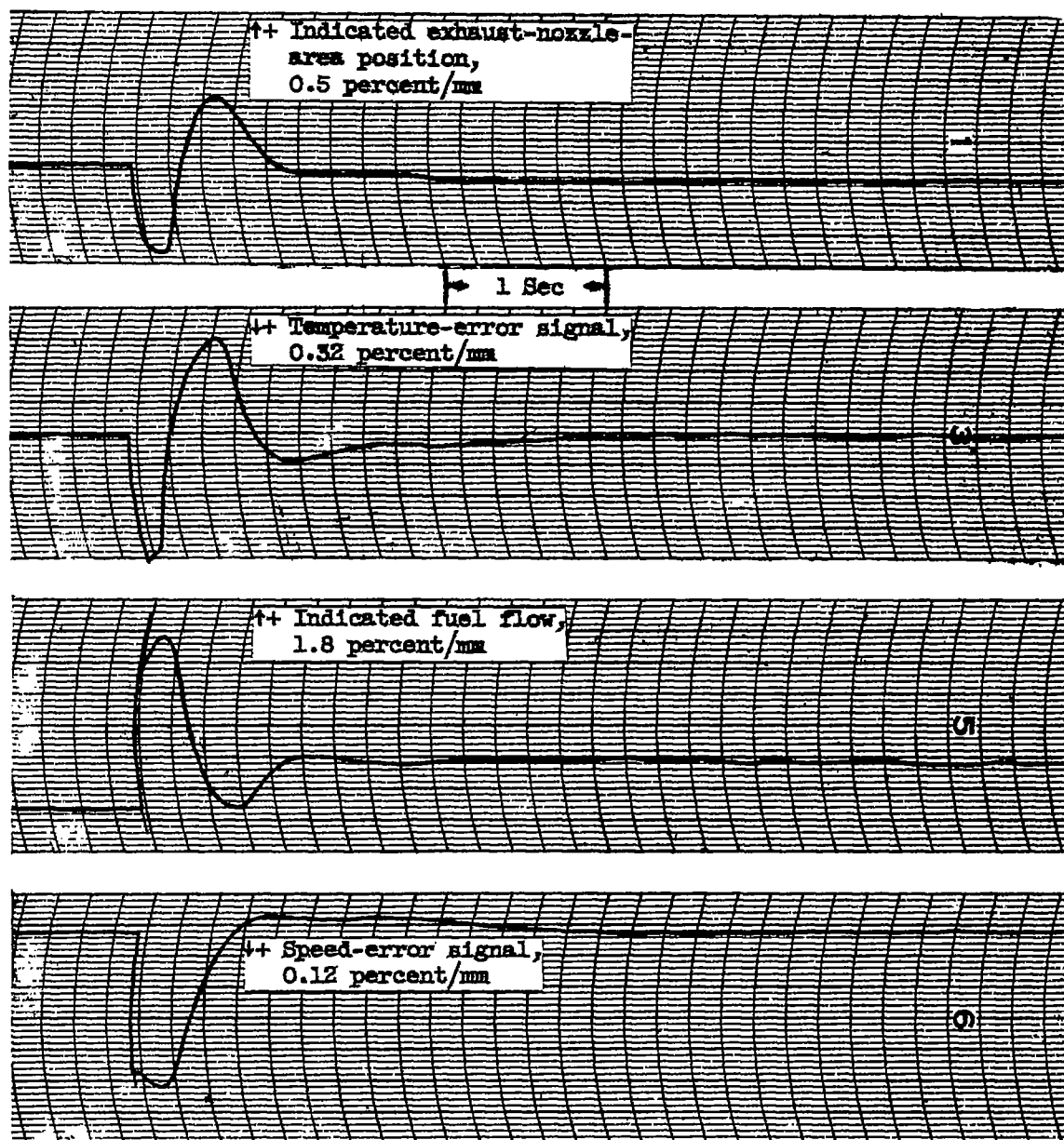


(a) Integral performance.



(b) Temperature and speed transient analyses.

Figure 9. - Speed - fuel-flow, temperature-area control system with temperature - fuel-flow compensation. Speed- and temperature-loop controller integrator settings, 0.5 second.



(c) Transient data. Speed-loop controller gain setting, 2.0; temperature-loop gain setting, 0.20.

Figure 9. - Concluded. Speed - fuel-flow, temperature-area control system with temperature - fuel-flow compensation. Speed- and temperature-loop controller integrator settings, 0.5 second.

4476

CF-7

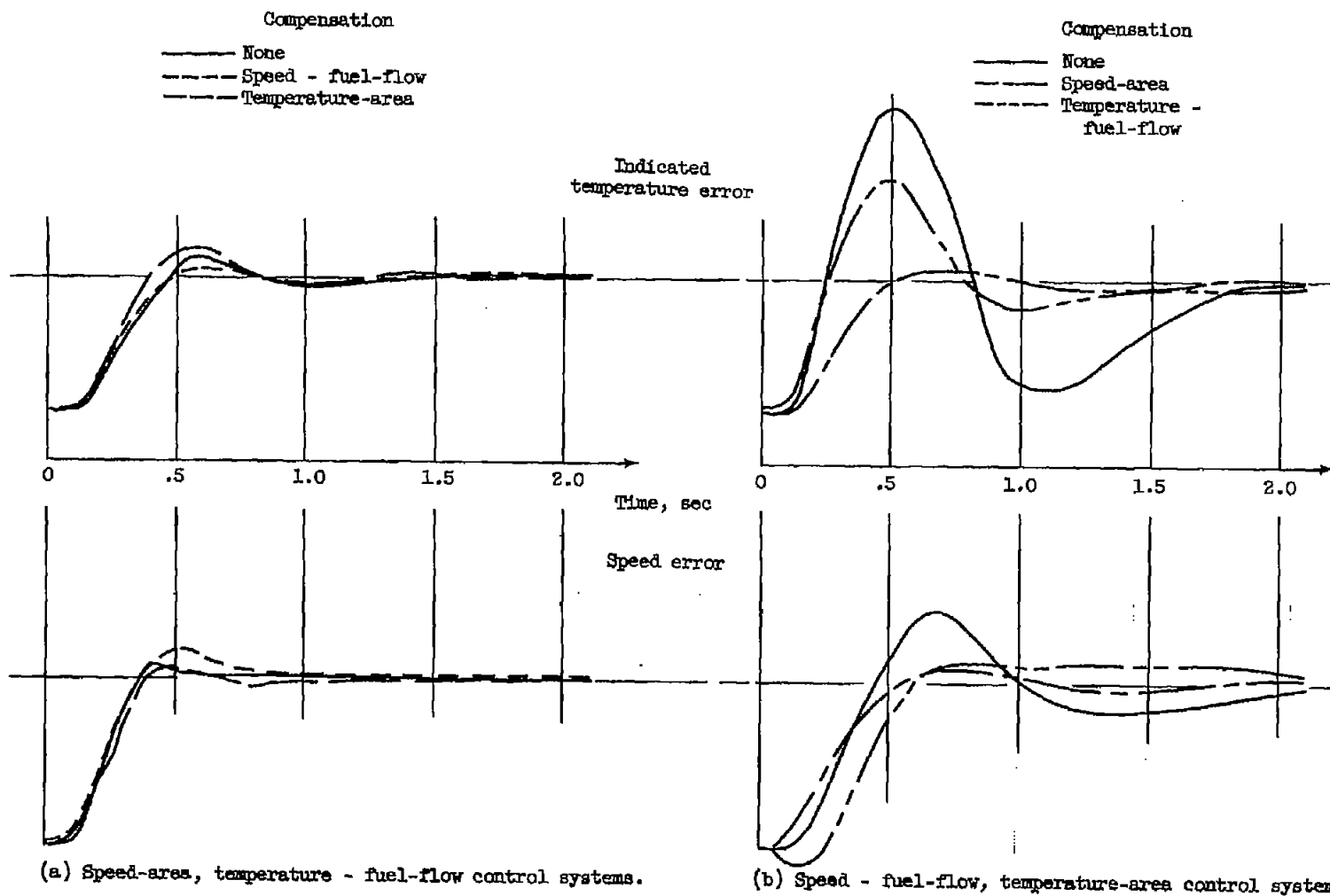
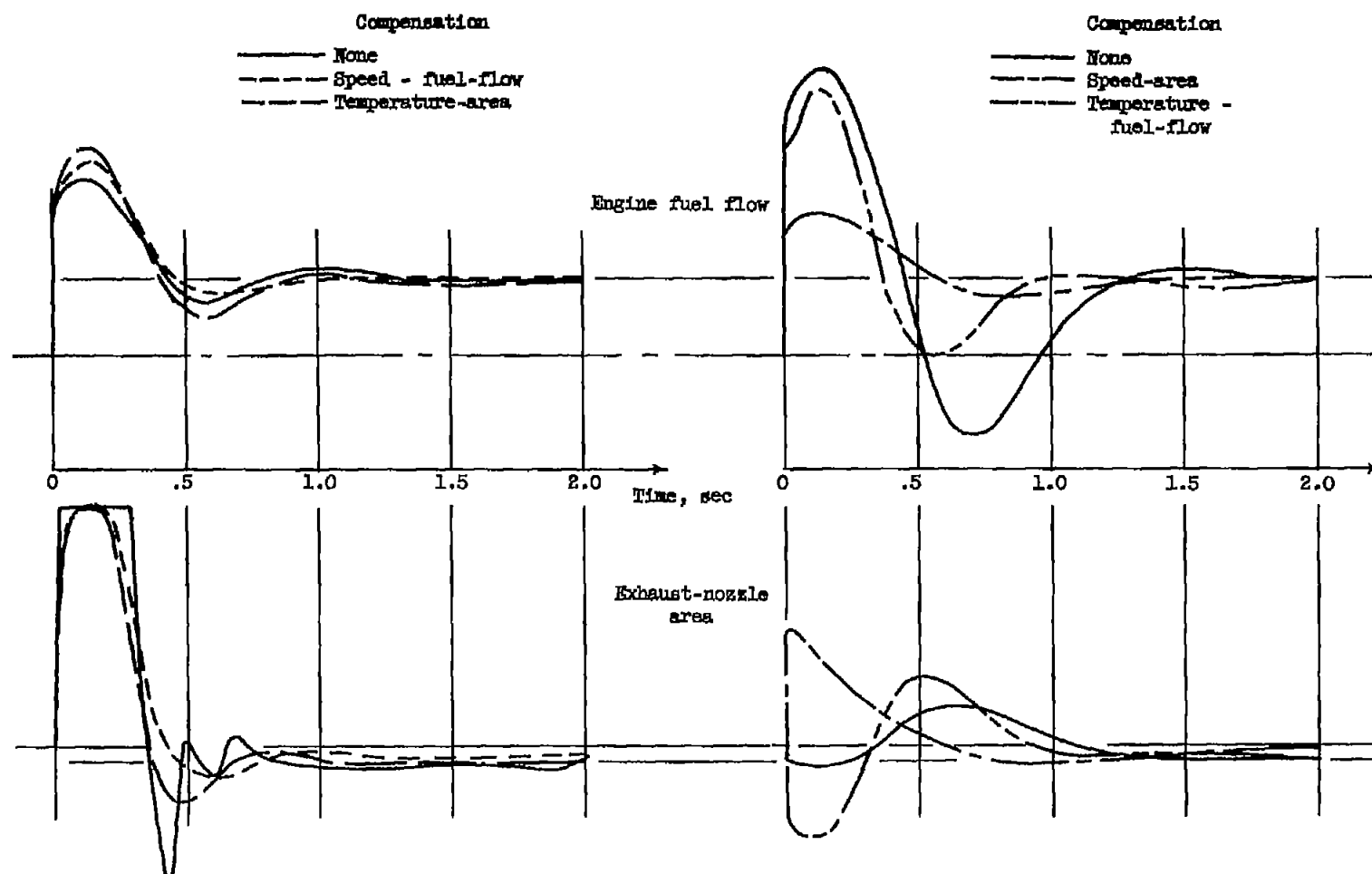


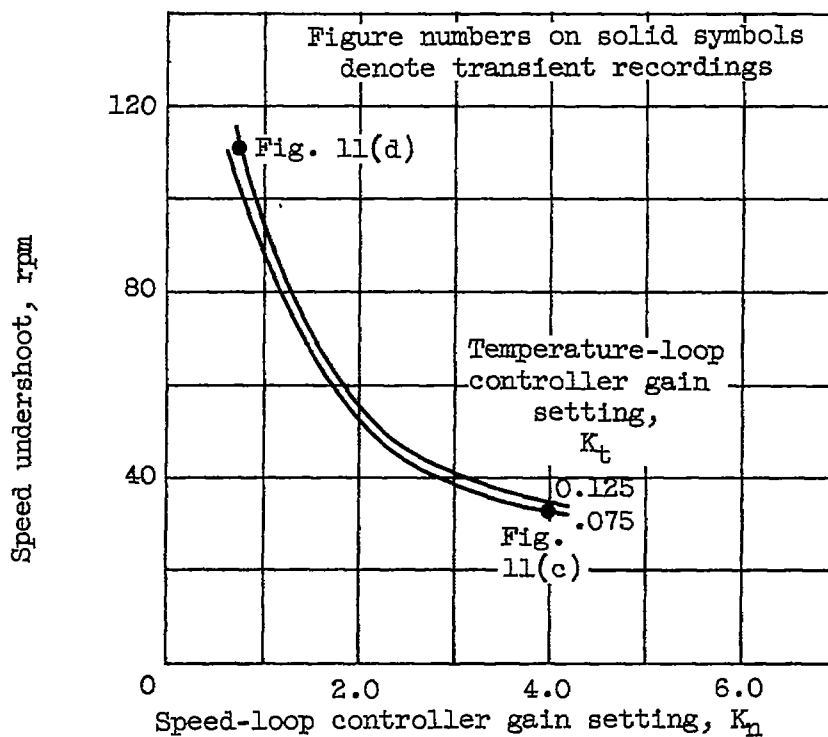
Figure 10. - Optimum response transients to simultaneous step increases in set speed and temperature for the six multiple-loop control configurations examined in this investigation.



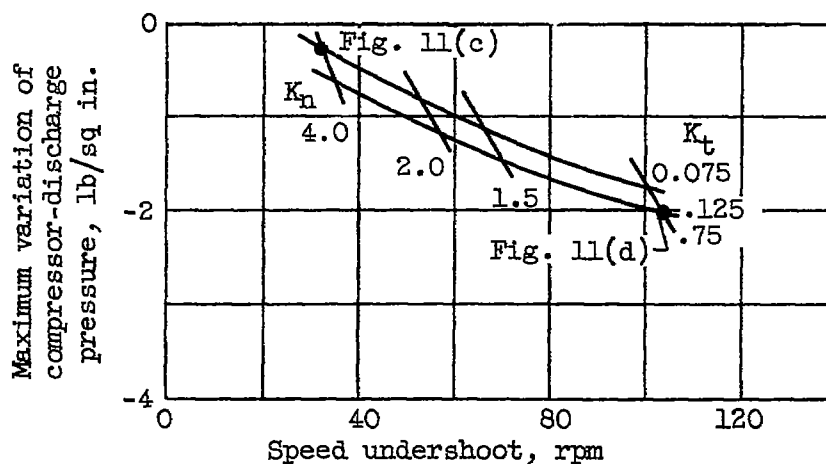
(a) Concluded. Speed-area, temperature - fuel-flow control systems.

(b) Concluded. Speed - fuel-flow, temperature-area control systems.

Figure 10. - Concluded. Optimum response transients to simultaneous step increases in set speed and temperature for the six multiple-loop control configurations examined in this investigation.



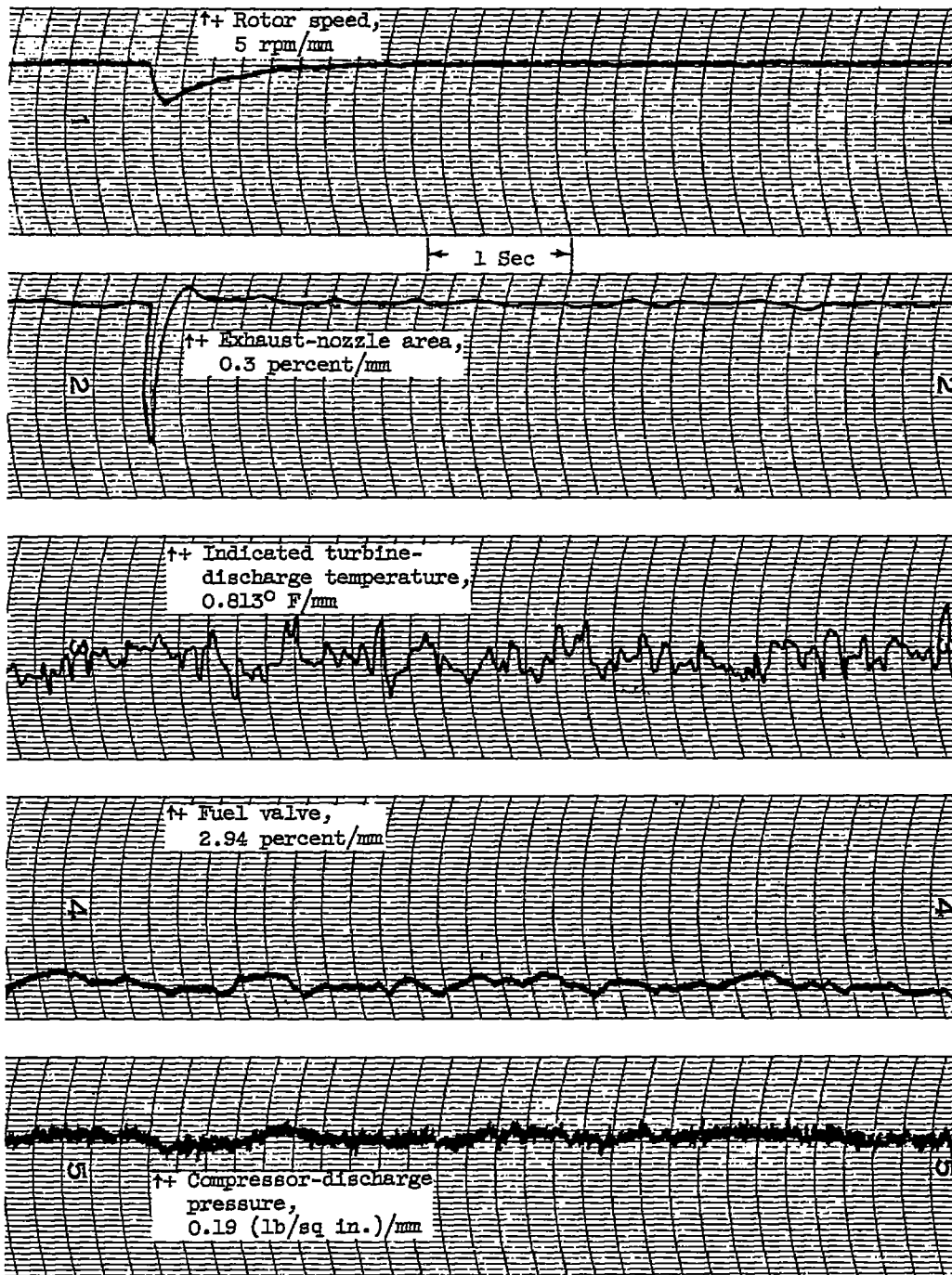
(a) Speed performance.



(b) Variation of maximum compressor-discharge pressure and speed.

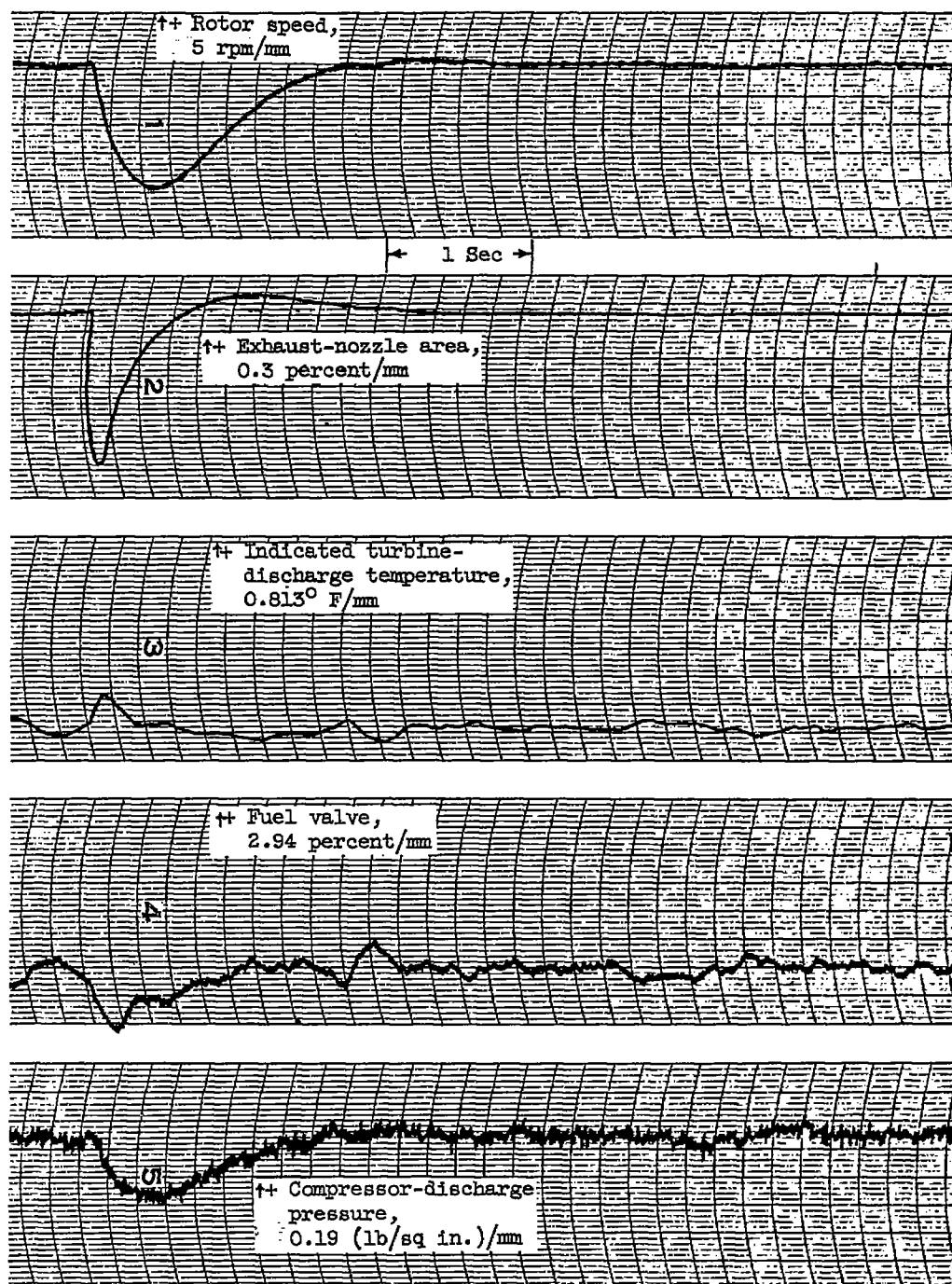
Figure 11. - Speed-area, temperature - fuel-flow control system with no compensation. Speed- and temperature-loop controller integrator settings, 0.5 second.

4476



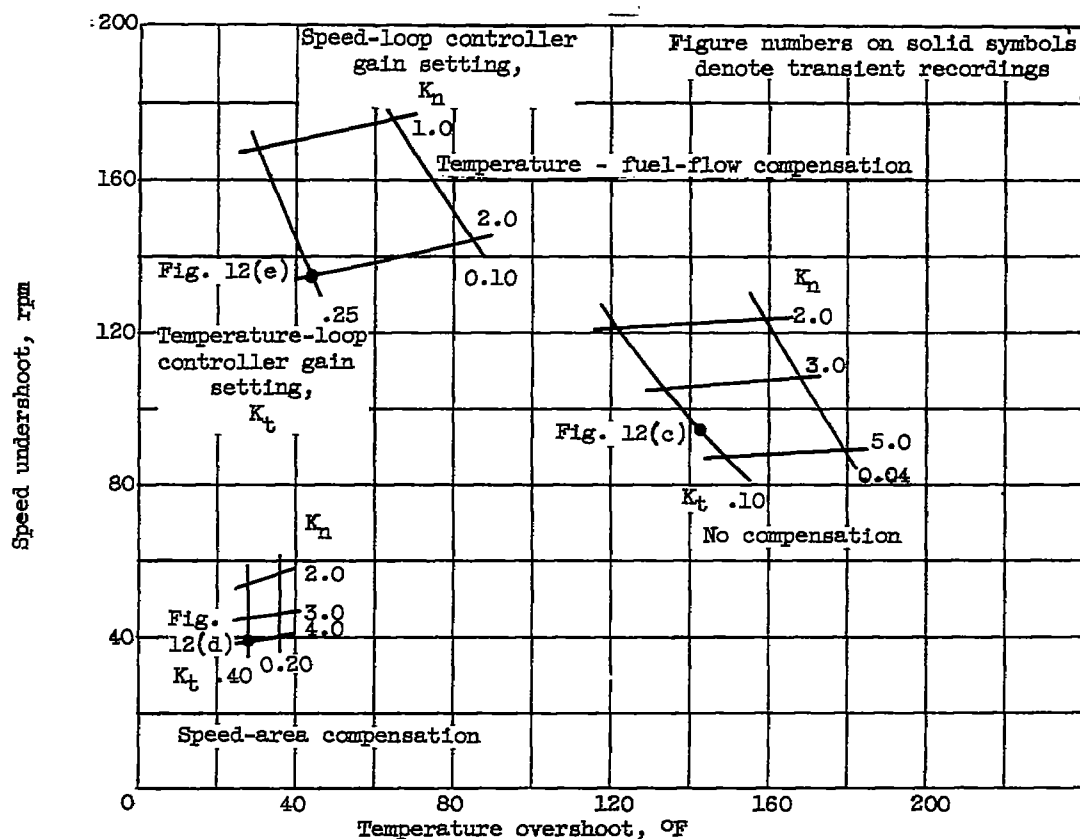
(c) Transient data. Speed-loop controller gain setting, 4.0; temperature-loop controller gain setting, 0.075.

Figure 11. - Continued. Speed-area, temperature - fuel-flow control system with no compensation. Speed- and temperature-loop controller integrator settings, 0.5 second.

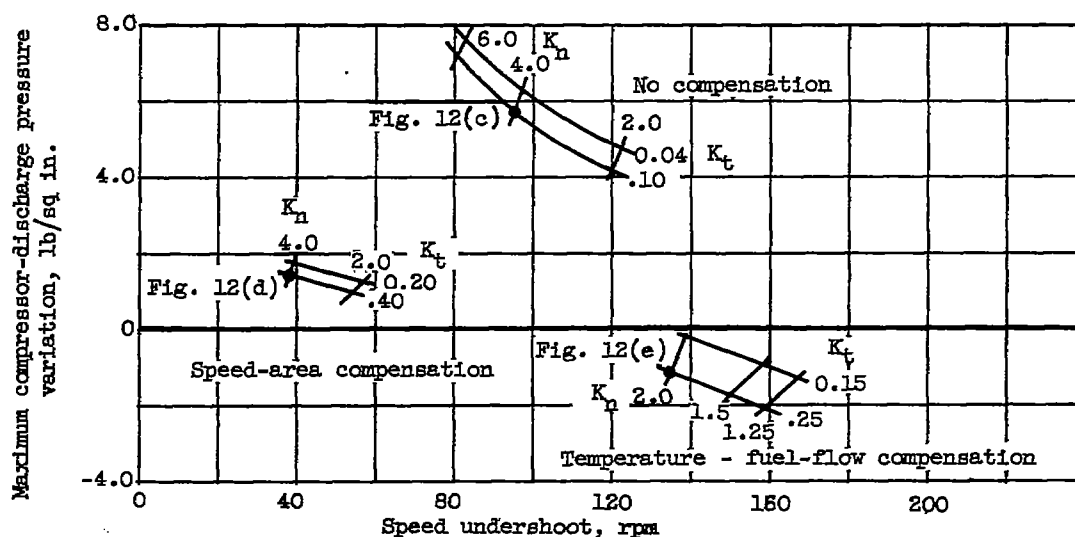


(d) Transient data. Speed-loop controller gain setting, 0.75; temperature-loop controller gain setting, 0.125.

Figure 11. - Concluded. Speed-area, temperature - fuel-flow control system with no compensation. Speed- and temperature-loop controller integrator settings, 0.5 second.

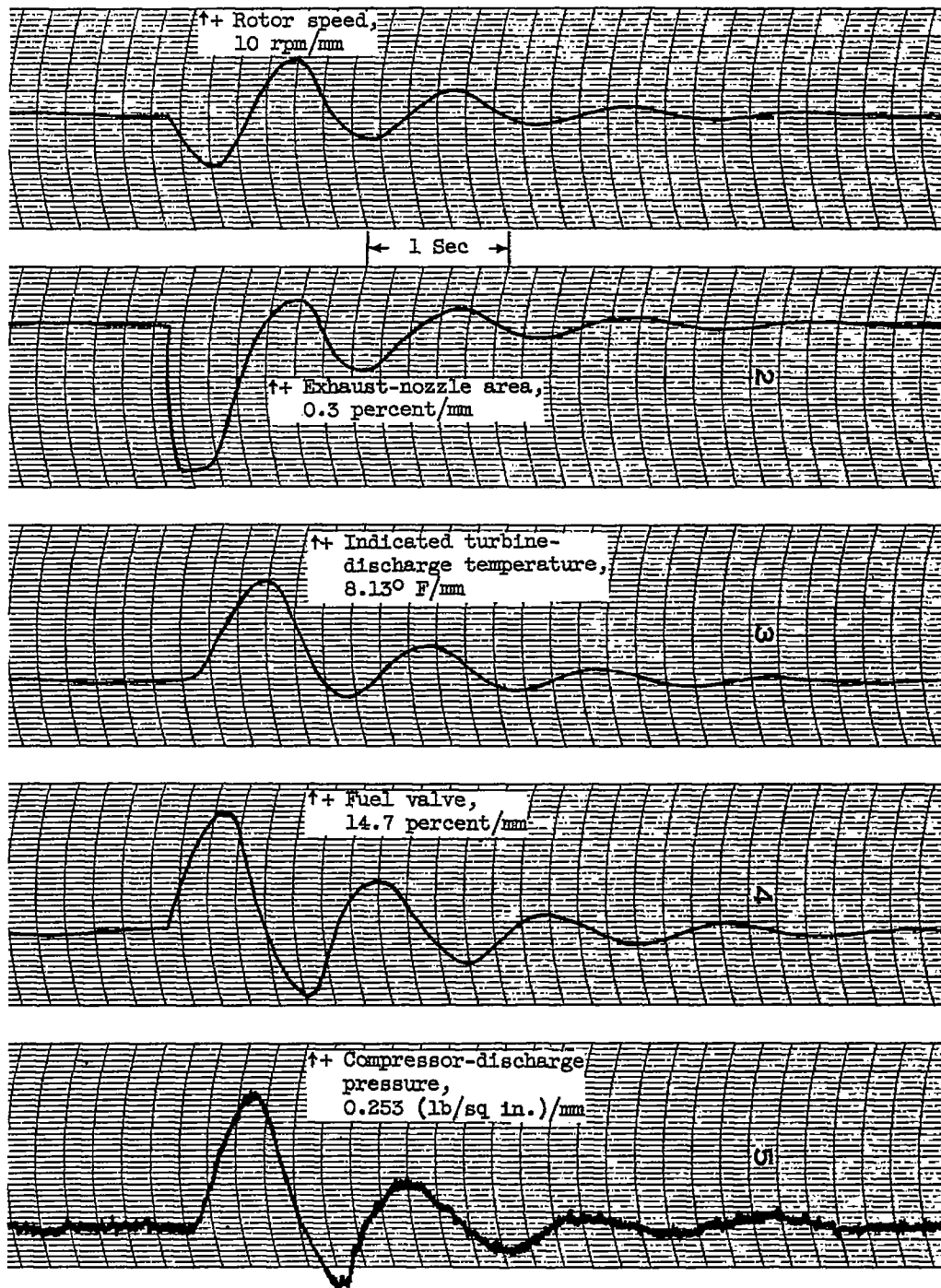


(a) Speed-temperature performance.



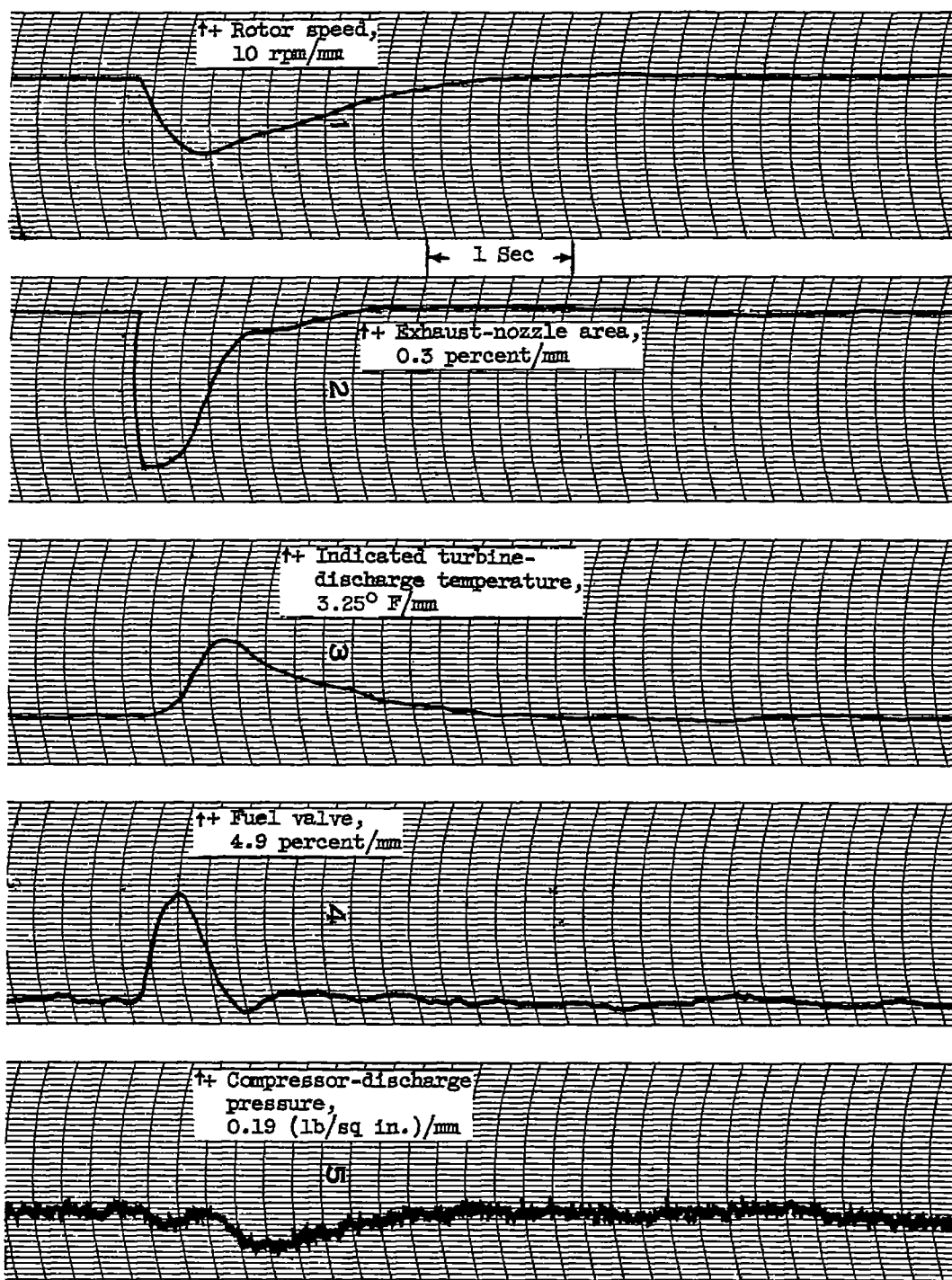
(b) Variation of maximum compressor-discharge pressure and speed.

Figure 12. - Speed - fuel-flow, temperature-area control systems.



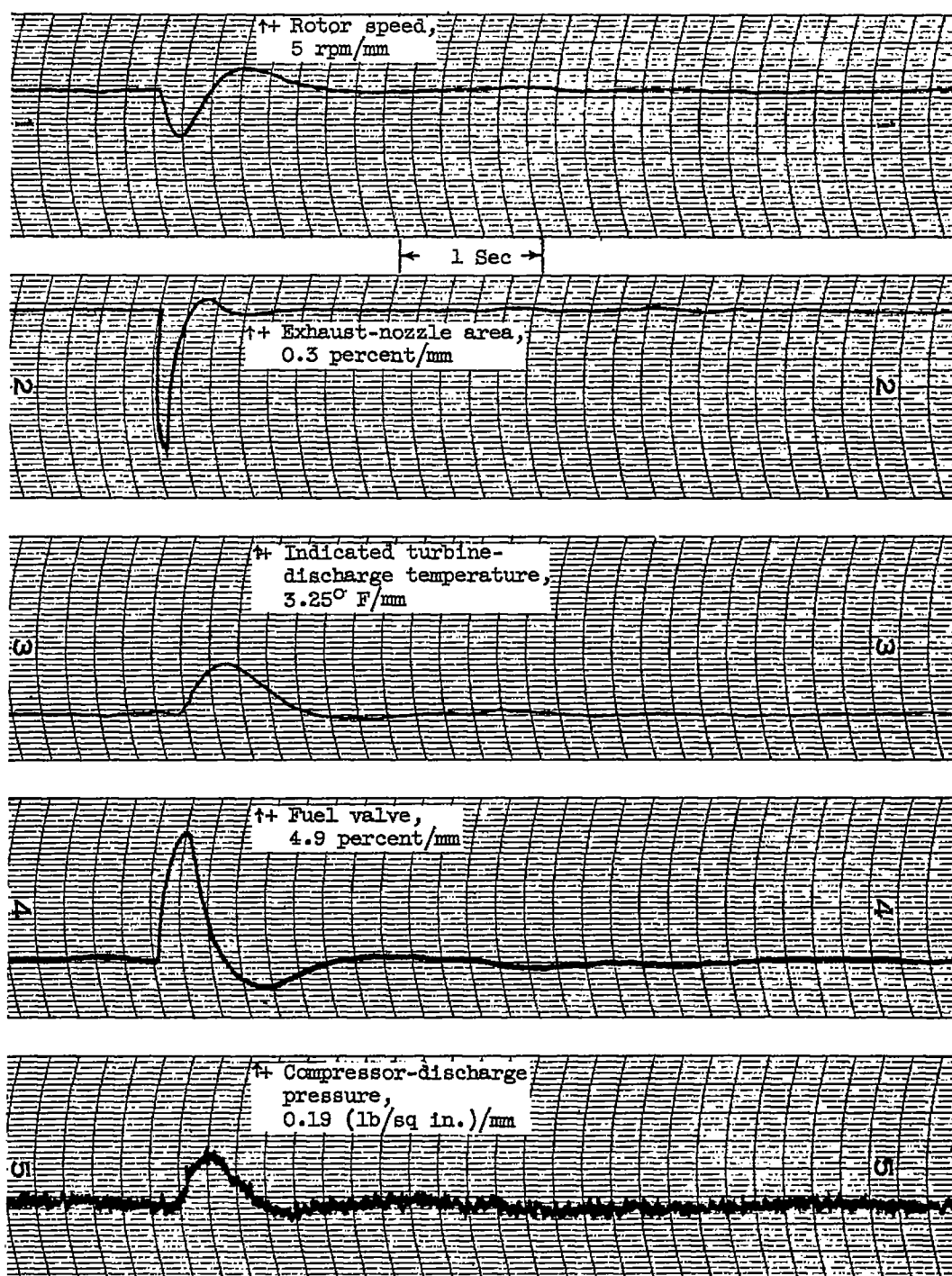
(c) Transient data. Speed-loop controller gain setting, 4.0; temperature-loop controller gain setting, 0.10; speed-loop controller integrator setting, 1.0 second; temperature-loop controller integrator setting, 0.25.

Figure 12. - Continued. Speed - fuel-flow, temperature-area control systems.



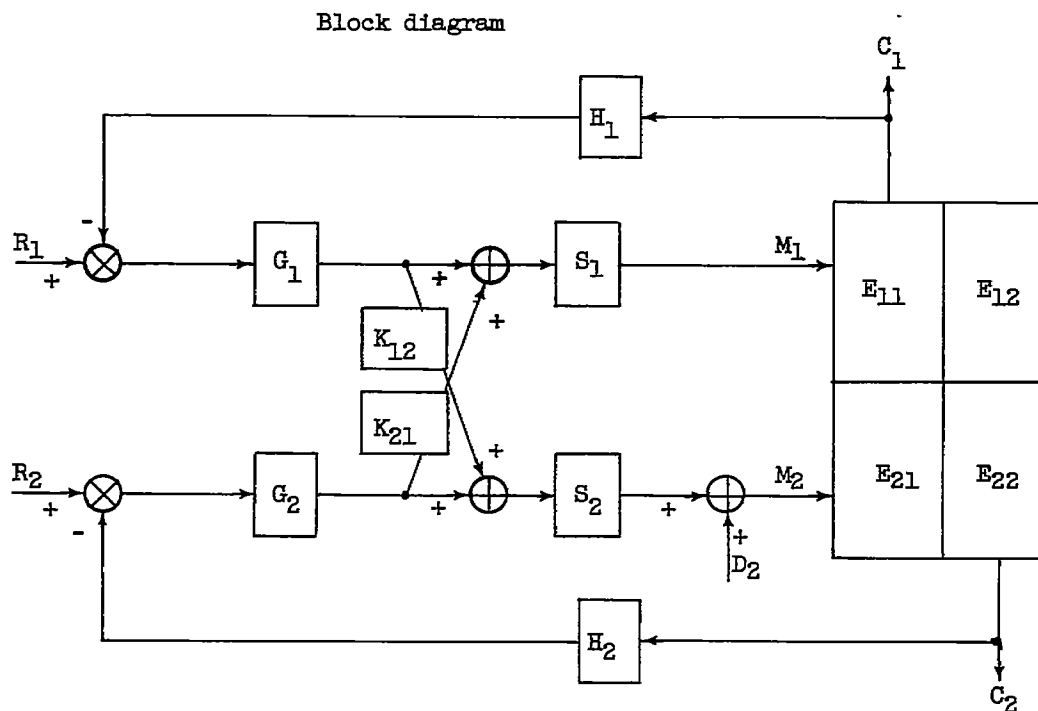
(d) Transient data. Speed-loop controller gain setting, 2.0; temperature-loop controller gain setting, 0.25; speed- and temperature-loop controller integrator settings, 0.5 second.

Figure 12. - Continued. Speed - fuel-flow, temperature-area control systems.



(e) Transient data. Speed-loop controller gain setting, 4.0; temperature-loop controller gain setting, 0.40; speed-loop controller integrator setting, 0.5 second; temperature-loop controller integrator setting, 0.25 second.

Figure 12. - Concluded. Speed - fuel-flow, temperature-area control systems.



System response equations

	$C_1$	$C_2$
$R_1$	$\frac{\frac{1}{H_1} [L_1(1 + L_2) - XY]}{\Delta}$	$\frac{\frac{1}{H_1} (Y)}{\Delta}$
$R_2$	$\frac{\frac{1}{H_2} (X)}{\Delta}$	$\frac{\frac{1}{H_2} [L_2(1 + L_1) - XY]}{\Delta}$
$D_2$	$\frac{E_{12}(1 + L_2) - E_{22}X}{\Delta}$	$\frac{E_{22}(1 + L_1) - E_{12}Y}{\Delta}$

$$\Delta = (1 + L_1)(1 + L_2) - XY$$

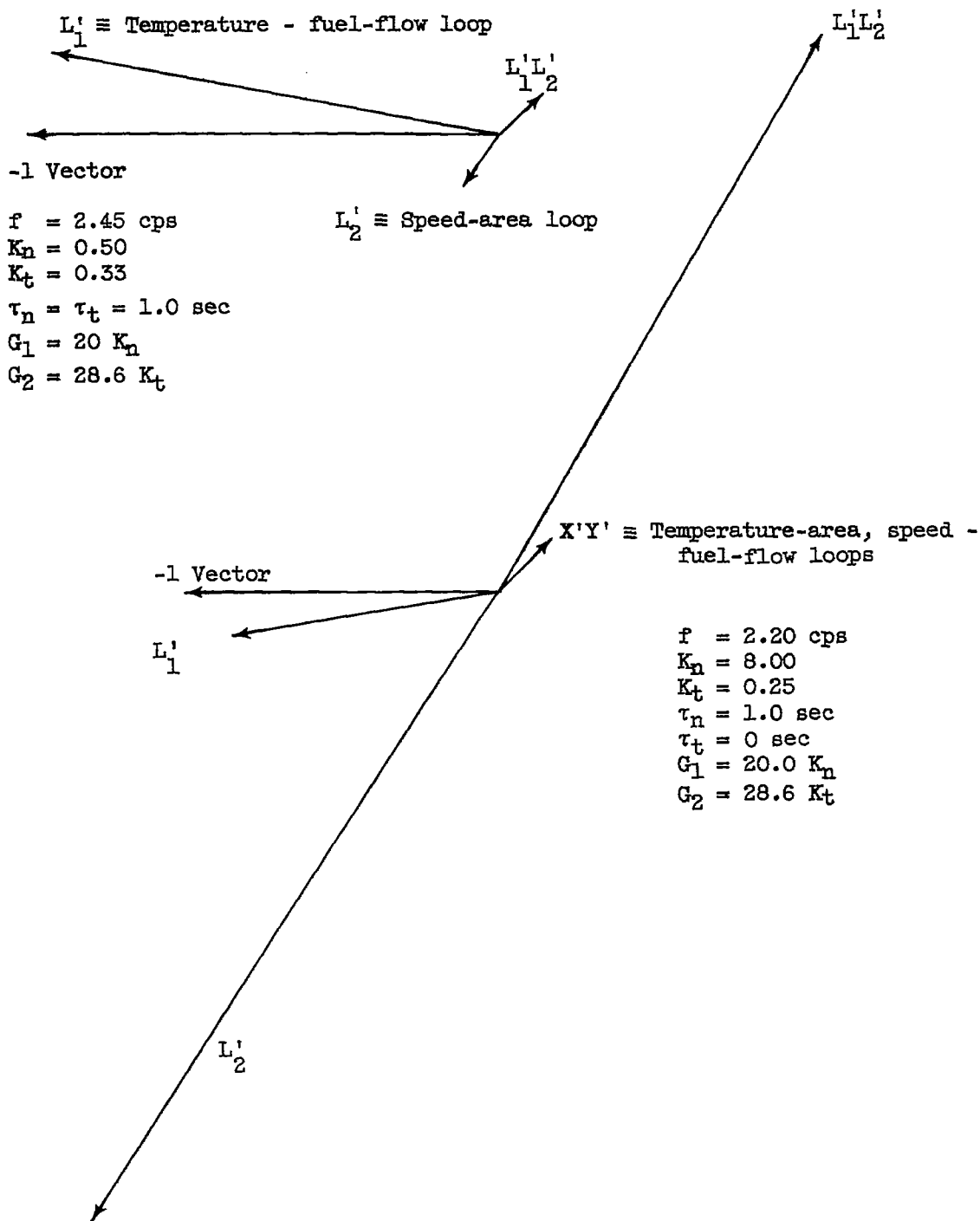
$$L_1 = G_1 S_1 E_{11} H_1 + G_1 K_{12} S_2 E_{21} H_1$$

$$L_2 = G_2 S_2 E_{22} H_2 + G_2 K_{21} S_1 E_{12} H_2$$

$$X = H_2 G_2 S_2 E_{21} + H_2 G_2 K_{21} S_1 E_{11}$$

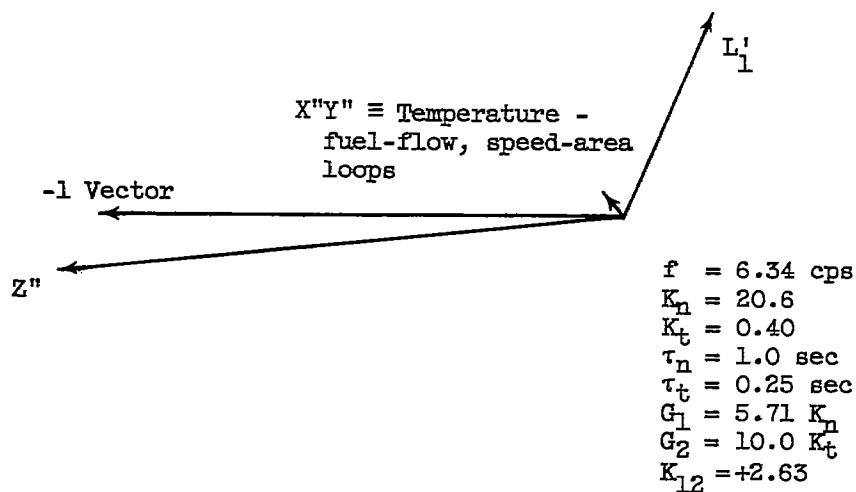
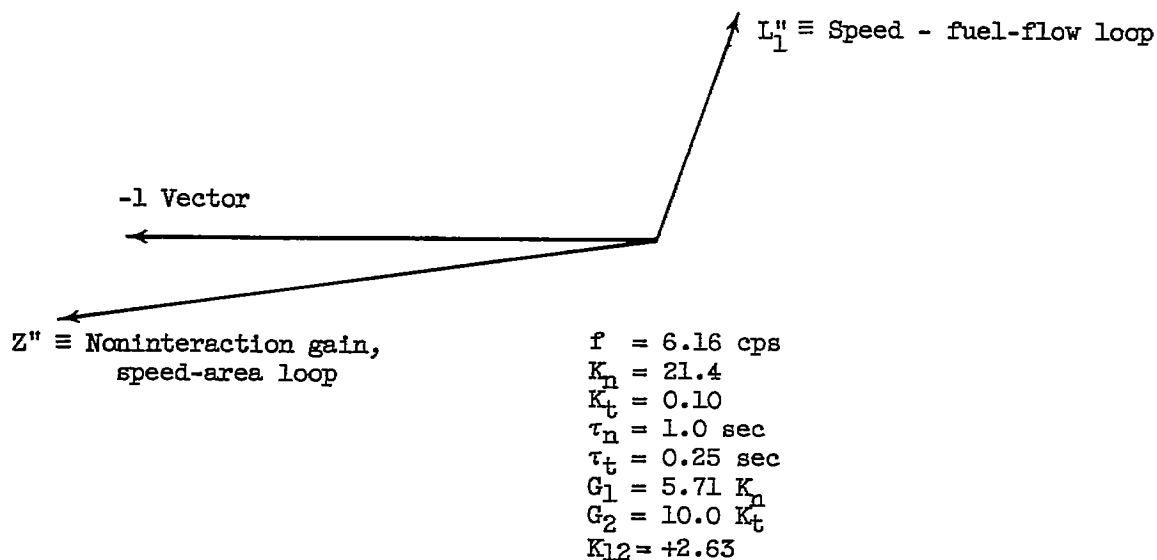
$$Y = H_1 G_1 S_1 E_{12} + H_1 G_1 K_{12} S_2 E_{22}$$

Figure 13. - Response equations for double-loop interacting control system.



(a) Speed-area, temperature - fuel-flow control configuration with no compensation.

Figure 14. - Vector diagrams of system characteristic equation at instability as function of controller gain settings.



(b) Speed - fuel-flow, temperature-area control configuration with speed-area compensation.

Figure 14. - Concluded. Vector diagrams of system characteristic equation at instability as function of controller gain settings.